

Formation and Properties of Magnetic Biochar

Nwosu Obinnaya Chikezie Victor (✉ nch015@uit.no)

UiT The Arctic University of Norway <https://orcid.org/0000-0003-3974-4755>

Research Article

Keywords: Magnetic biochar, SRC willow, Agricultural biomass, Metal pollutants, Copper, X-ray diffraction

Posted Date: October 18th, 2022

DOI: <https://doi.org/10.21203/rs.3.rs-2112623/v1>

License: © ⓘ This work is licensed under a Creative Commons Attribution 4.0 International License.

[Read Full License](#)

FORMATION AND PROPERTIES OF MAGNETIC BIOCHAR

Nwosu Obinnaya Chikezie Victor

UiT The Arctic University of Norway

PO Box 6050 Langnes

N-9037 Tromsø

Norway

Nch015@uit.no

ABSTRACT

Magnetic biochar made from agricultural biomass waste such as SRC willow, which is a densely planted, high-yielding energy crop and one of the leading sources of renewable energy production, combined with iron (II) chloride and iron (III) chloride, is a multi-functional material for land remediation and agricultural applications. Two magnetic biochar's (1.0 M iron solution magnetic biochar and 0.1 M iron solution magnetic biochar) were prepared by the chemical mixture and co-precipitation of iron (II) chloride tetrahydrate and iron (III) chloride on SRC willow with a particle size of less than 2 mm (about 0.08 in). The mixture of SRC willow with iron (II) chloride tetrahydrate and iron (III) chloride was then dried in the oven and pyrolyzed at 400 degrees Celsius. Scanning electron microscopy, Fourier transform infrared spectroscopy, and X-ray diffraction research on the 1.0 M iron solution magnetic biochar and the 0.1 M iron solution magnetic biochar reveal a greater concentration of iron compounds in the 1.0 M iron solution magnetic biochar. Ultraviolet infrared spectrometry was performed on iron (II) chloride tetrahydrate, iron (III) chloride, and copper (II) sulphate pentahydrate. Atomic absorption spectroscopy and ultra-violet spectrometry were performed on copper (II) sulphate pentahydrate and deionized water mixed with 1.0 M iron solution magnetic biochar, 0.1 M iron solution magnetic biochar, and activated for atomic absorption spectroscopy, 0.1 M iron solution magnetic biochar has a greater adsorption capacity than 1.0 M iron solution magnetic biochar for copper (II) sulphate pentahydrate solution. For ultra-violet infrared spectroscopy, the adsorption capacity of magnetic biochar in a 1.0 M iron solution is greater than that of magnetic biochar in a 0.1 M iron solution. Based on these results, both the 1.0 M iron solution magnetic biochar and

the 0.1 M iron solution magnetic biochar are good options for removing metal pollutants like copper and restoring land.

KEYWORDS

Magnetic biochar; SRC willow; Agricultural biomass; Metal pollutants; Copper; X-ray diffraction

1.0 GENERAL INTRODUCTION

1.1 BACKGROUND

This study focuses on the synthesis and characteristics of magnetic biochar, which is used for the restoration of soil contaminated by metallic poisons and pollutants. Magnetic Biochar is a type of biochar or charcoal that looks like potting soil and is mixed with an iron solution. It is made by heating up biological waste, and it is used to store massive amounts of carbon from the air in the soil (Bracmort, 2009). It is also charcoal in its stable form, which is created by applying heat to organic material combined with a magnetic substance at a maximum temperature in the absence of oxygen or with extraordinarily little oxygen via pyrolysis. The biochar generation from pyrolysis generates syngas, which is a synthetic gas comprised of several gases that are captured and used to produce energy (Krull). The carbon cycle and climate change are the methods by which carbon migrates across the Earth's systems, illustrating how carbon and weather change are regulated by the earth's systems and how carbon is moved from one form to another. Also, the carbon flow through the carbon cycle illustrates the management of climate change and greenhouse gases by the biosphere, atmosphere, hydrosphere, and geosphere of the planet (Bennington, 2009). The purpose of this thesis is to produce magnetic biochar via chemical co-precipitation and pyrolysis at different temperatures and to characterize the physical, chemical, and formation of magnetic biochar via Fourier transform infrared spectroscopy, X-ray diffraction, and transmission or scanning electron microscopy. In an experiment to assess the adsorption analysis of magnetic biochar, copper sulphate was used. This process of making magnetic biochar will be used to remove metal poisons and soil contaminants by absorbing them and cleaning them up.

2 LITERATURE REVIEW

2.1 EXPLANATION OF BIOCHAR

The research line has been divided into four broad sections for this thesis: the explanation of biochar and why it is interesting; the explanation of how biochar is produced; the current and potential future applications of biochar; and the science behind magnetic biochar and why it is interesting. Biochar is a novel material discovered in soils across the world because of environmental occurrences that are prevalent west of the Mississippi River and east of the Rocky Mountains, where most of the the world's productive and rich soils are situated. There is evidence that biochar is present in fertile soils known as "Terra Preta" and "Terra Mulata" in the Amazon basin, which translates to "Dark Soil" in Portuguese. These soils were created by ancient Amazon cultures, and because of the copious quantities of biochar found in the soils, the region is still very fertile due to the increased rate of leaching caused by rainfall. Also, in Asian areas of the globe, biochar usage in agricultural operations has a long history that has lately led to the development of advantageous agricultural systems and practices (Hunt et al., 2010). Laboratory analyses of the "Terra Preta" have revealed elevated concentrations of organic materials and bio coal, such as the remains of animals and plants; its high level of productivity is due to its favorable retention of nutrients and good pH for acidic soils; and these "dark soils" are found in places of human settlement that were created by the ancient technique of slash-and-char, which entails removing vegetation from a small area and setting it on fire, allowing the resulting charcoal to accumulate (Talberg, 2009). The Terra Preta is renowned for its high bio coal or charcoal content, which is a mix of organic debris, charcoal, and animal droppings added over a period of years to the barren soils of the Amazon. This serves to enable a rise in microorganism activity, which is important for plant development and reduces soil nutrient leakage, which is a severe issue in tropical rainforests. Soil investigations have shown that the Terra Preta era began about 450 B.C., depending on the location of the soil (Robert, 2011). In the early 1500s, the first European, Francisco (Organic arsenic adsorption onto a magnetic sorbent, 2009) de Orellana, visited the Central Amazon and reported to the Spanish court on the discovery of a vast agricultural civilization along the Amazon

banks. On the German island of Sylt, the first manufactured soils to be enhanced with organic matter (biochar) from heathlands date back as far as three thousand years (F.Verheijen, 2010). Also, Wim Sombroek, a Dutch soil scientist, established Terra Preta in the middle of the 20th century, which comprises 10 per cent of the Amazon Region and is in Liberia, the Benin Republic, Peru, and Ecuador (Bio11). In his book "Amazon Soils" from 1966, Wim Sombroek talks about the science and research behind "terra preta." Also, Bruno Glaser from the University of Bayreuth in Germany demonstrates that crop productivity on terra preta is two times greater than on plain soils. This is due to the agric-char that makes organic material undergo a smouldering process in a no oxygen or oxygen-deficient condition, allowing the biochar to collect water and nutrients that are washed down to the roots, housing a micro-organism community that makes the soil darker in colour and According to the findings of Bruno Glaser, a hectare of terra preta with a depth of one meter contains between two hundred and fifty tons of carbon compared to one hundred tons on the unfertile ground with the same parent material. Also, Johannes Lehmann, the first author of the book "Amazonian Dark Earths: Origin, Properties, Management," from Cornell University, New York, stated that by the end of the century, the Terra Preta programmed mixed with biofuel can sequester approximately 9.5 billion tons of carbon annually and that the enriched soil was created by human settlements using the slash-and-char processes, which are low-intensity smouldering fires that are covered with waste, excluding organic matter (2006). In 1879, Herbert Smith nurtured Scribner's Monthly with stories about the Amazon covering every detail, such as the splendid growth of the sugar plantations, whose secret was the extraordinarily rich and fertile "terra preta" soils, which were the best type of soils in the Amazon and had the characteristics of being dark loam, fine, and two feet thick. William Woods, a retired human settlement professional from the University of Kansas, collected "terra preta" samples from the Amazon region of Brazil, which contained up to nine per cent carbon compared to the 0.5% of regular soil from nearby regions. Robert Brown asserts that a 250-hectare biochar-ammonium-nitrate farm can store more than 1,900 tons of carbon per year (2006). Christopher Steiner from the University of Georgia suggested that the production of agrichar from chicken manure may assist in creating extremely productive sandy soils. David Laird argues that agrichar may benefit the enriched soil of the Midwestern United States by minimizing the leakage of soil nutrients and by removing carbon dioxide from the Earth's atmosphere, which is currently considered a severe issue (Honcho, 2010). The Amazon Terra Preta de Indio demonstrates that unproductive soils may be transformed into productive

soils, hence reducing the need for fertilizer and influencing the environmental consequences of agricultural soils. [The11]. Biochar soils have a significant decrease in nitrous oxide emissions and phosphorous discharge, and the magnetic biochar process reverses land degradation in polluted, depleted, and organic matter-deficient regions. Trimble noted in the 19th century that the influence of charcoal dust on farms in his nation led to an increase in flora. In the 20th century, Retan and Tryon conducted research on the influence of agrichar on seedling development and the chemical properties of soil, which provides scientific knowledge on biochar. In Japan, biochar research increased in the early 1980s. In the early 20th century, Morley wrote in "The National Green Keeper" that biochar holds gases, solutions, and water in the soil like a sponge. He added that biochar is unmatched as a soil cleaner and moisture absorber, and biochar products are available on the market. Young introduced a parking and burning technique in 1804 in which soils are piled with organic debris, such as peat, and then put on fire to boost their agricultural value. Also, according to Justus Liebig, biomass was combined with soil and burned until black soil was produced, which helped plant growth in China. According to Ogawa, Miyazaki described agrichar as "fire-made manure" during the ancient Japanese agricultural era of the 17th century (Johannes, 2009). During the advent of metallurgy, circa 3000 B.C., biochar was employed to achieve temperatures above one thousand degrees Celsius while producing minimal smoke, which is advantageous for smelting. Copper ore oxides are reduced by biochar. The earliest biochar was formed by the slow combustion of wood in a pit filled with dirt, which was widespread in 20th-century Europe. Carl W. Scheele, a Swedish scientist from the 18th century, was the first to investigate the absorptive properties of biochar. Biochar was used to change soil at the end of the 19th century. Professor Charles Hart and his student, Herbert H. Smith, brought Amazon Dark Soils to the attention of scientists. The Amazon Dark Earth has been around since pre-Columbian times. The biochar shoal has high nutrient holding retention due to carboxylic due to apparent degeneration, has a high pH value, and holds copious quantities of H₂O, and the agrichar polycyclic ambrosial design counteracts elemental putrefaction and synthetic degeneration, which illustrates its tenacity in the atmosphere (Meyer, 2009). This was achieved by Zhejiang Provincial Key Laboratory of Organic Pollution Process and Control, Zhejiang University, China, through chemical co-precipitation of iron ions on a biomass material and high-temperature pyrolysis. (A novel magnetic biochar efficiently sorbs organic pollutants and phosphates, 2010). Terra preta is abundantly rich in potassium, calcium, zinc, phosphorus, and manganese, but most notably

charcoal, which gives rise to the dark colour of terra preta. The charcoal form in the Terra preta soil is distinct from that produced traditionally as a source of cooking fuel; the chemical orientation of biochar consists of a poly-structured aromatic presence that protects against microbial decomposition (Rodriguez et al., 2009). Rosalind Franklin published a paper on biochar structures in which she proposed a 65 per cent model of carbon stored in graphite, demonstrating the main difference between coke and char by demonstrating that coal obtained from coke is transformed into transparent charcoal at elevated temperatures, whereas biochar cannot be converted to sludge. In the late 1970s, the quantum physicist Freeman Dyson initiated a project to improve carbon sequestration in plants and soil, which slows the rise of carbon dioxide in the atmosphere and substitutes fossil fuel with biofuel. Also, biochar is the residue from biomass heated in the absence of oxygen, which undergoes a chemical transformation during heat application to create a benzene ring arrangement that is difficult for microorganisms to attack. Karve (2009) explains that biochar can be used to promote the health of the soil and the growth of vegetation. Biochar is used in soil amendment and increases agricultural productivity for farmers, making its explanation intriguing. In addition, it is used to manage soil quality, mitigate climate change, and provide further environmental advantages. (The African Biodiversity Network, 2009) Biochar is a very fine-grained charcoal formed from biomass conversion by pyrolysis that is applied to soils; biomass is "cooked" at elevated temperatures in the absence or restricted availability of oxygen. Fuels generated from pyrolysis are used as agrofuels for automobiles and aircraft (Organic arsenic adsorption onto a magnetic sorbent, 2009). Biochar is a carbon-porous solid created by the thermochemical conversion of organic materials in the absence or presence of oxygen. It is very stable and is used for long-term carbon storage in the soil, carbon emission reduction, and soil enhancement. When biomass (such as wood, dung, or agricultural waste) is roasted in an enclosed container with limited air, it is converted into biochar, which is then put on tropical soils to increase crop productivity. (Speeding, 2010). It is a form of black charcoal that is produced when natural organic materials such as crop wastes, timber, and litter are heated in the absence of oxygen, and it is receiving a great deal of attention as a fertilizer, soil conditioner, and carbon store. The biochar produced depends on the material being burned, its temperature, and the heating process rate, so biochar made from the chicken litter will have a different nutrient content than biochar made from timber.

In addition, the adsorption properties of biochar generated at 700 degrees Celsius vary from those formed at 400 degrees Celsius (Quayle, 2010). It is the byproduct of cellulose matter that has undergone thermal treatment, such as gasification, pyrolysis, or hydrothermal carbonization, in the presence of a restricted supply of oxygen, resulting in the production of oil and gas for heating and energy production. Biochar is a potential future invention used to reduce emissions and enhance soil quality (Ernsting, 2009). Biochar combined with fly ash can be used to develop terrestrial carbon storage on underutilized land as well as to change soil properties such as porosity, pH, water-holding capacity, conductivity, dissolved sulphates, carbonate, and chloride anions and cations (Palumbo et al., 2009). It is formed by the thermal process of biomass under reduced oxygen conditions; its addition improves cation exchange capacity, allowing for more effective plant nutrient delivery and water retention (Backer et al., 2011). Biochar produced from specific biomass consists of organic carbon with macro and micronutrient content for plants derived from the original feedstock; the composition of biochar is dependent on the kind of feedstock and pyrolysis circumstances. Biochar may have relative amounts of elements such as Sulphur, hydrogen, oxygen, bases, and heavy metals; biochar that is recently produced has graphene layers and aromatic structures as components. Biochar made by pyrolysis at low temperatures is acidic, while biochar made by pyrolysis at elevated temperatures is alkaline.

2.2 EXPLANATION OF BIOCHAR PRODUCTION

The ancient process of biochar formation is the result of forest fires and human-caused burning in pits; the resulting char is put on the soil as a soil amendment and is known as "BIOCHAR." Traditional charcoal production methods are not environmentally friendly. This ancient method of creating biochar originated in the Amazon Basin of South America, where humans would stack wood in earthen pits and burn it slowly in the lack or near absence of oxygen. Additionally, biochar is created using Klin technology. The kiln is composed of steel, brick, and dirt, but it may also emit smoke and other greenhouse gases that contribute to climate change on a worldwide scale. Moreover, biochar is produced by a pyrolytic process in which biomass is heated in the absence of oxygen at temperatures between 350 and 700 degrees Celsius in furnaces in which gases such

as syngas, oxygen, and hydrogen are either burned off or captured, and bio-oil is also produced, which is a major source of energy (Howl1). This is a thermochemical process that converts biomass into bio-oil, biochar, and carbon black. At temperatures exceeding 400 degrees Celsius and in the absence of oxygen, organic matter thermally decomposes into a vapours stage and a residual solid stage, which is the biochar; cooling of the vapours (i.e., high molecular-weight volatile chemicals) results in condensation, which is the bio-oil. This pyrolytic method is of two types: fast pyrolysis and slow pyrolysis. Fast pyrolysis occurs at temperatures around 500 degrees Celsius and produces char in a matter of seconds, ds, whereas slow pyrolysis occurs at temperatures below 400 degrees Celsius and requires more time to produce biochar in copious quantities. ECO Pyro-torrefaction is a regular flow heat circular process that is operated at approximately 500 degrees Celsius using a sophisticated mechanized non-oxygenated void reactor in which a heat-chemical transformation removes the erratic constituent of biomass matter, stabilizing the residue portion of the carbon into biochar and other products that accompany it (ECh11). In addition, we will discuss slow pyrolysis in general, which is the most prevalent applied science in biochar production. This is accomplished by applying heat ranging from twenty degrees Celsius per minute to one hundred degrees Celsius per minute at an elevated temperature of six hundred degrees Celsius to a biomass material to produce equal by-products since the time for vapours to disperse is sufficient for most of the biomass to be splintered. In addition, varieties of slow pyrolysis based on kiln technologies, such as drum pyrolyzes and screw pyrolyzes, exist (Martin, 2009). Gasification of biomass is the incomplete combustion of biomass matter that results in the production of carbon monoxide, hydrogen, and methane called "producer gas" or generator gas at temperatures up to 1,000 degrees Celsius in a gasifier; this gas can be used to run engines, produce furnace oil, and methanol (Rajvanshi). Flash pyrolysis is a method of treating biomass to produce high oil yields of up to 75%; the process is distinguished by rapid heating rates, higher temperature values ranging from 450 to 600 degrees Celsius, and a short gas residence time at elevated temperatures. This technique produces bio-oil with a fivefold greater energy density than its biomass, and the oil may be stored and delivered (Bramer). Hydrothermal carbonization is the rapid method of biochar generation in the presence of water in which biomass is heated in water at around 350 degrees Celsius under pressure for one hour. Hydrothermal carbonization converts wet biomass into solid carbon at high yields without the need for an intensive drying procedure (Sorption of bisphenol A, 17 alpha-Ethinyl estradiol, and phenanthrenes on thermally

and hydrothermally generated biochar, 2011). Rice hulls and corncobs with high adsorption capacity are produced by rapidly pyrolyzing biomass in a pyrolysis reactor. (Preparation of biochar with a high absorption capacity from waste biomass, 2011) Biochar produced from rice hulls and legumes decreases soil acidity and increases soil alkalinity, hence enhancing soil fertility and liming potential (Amendment of Acid Soils with Crop Debris and Biochar, 2011). In a fluidized bed reactor, chicken litter is transformed into biocrude oil, which is then utilized for energy production (Biocrude oils from the quick pyrolysis of poultry litter and hardwood, 2009). Oak bark biochar is produced by the rapid pyrolysis of oak wood in an auger reactor; the biochar produced is used for the removal of chromium from water, for which the adsorption isotherm has been determined (Modeling and evaluation of chromium remediation from water using low-cost biochar, a green adsorbent, 2011). Product yield from pyrolysis varies with temperature, with lower temperatures producing more biochar per unit of biomass and higher temperatures producing more syngas per unit of biomass. The three primary methods for deploying a pyrolysis system are as follows: the first is a centralized process system in which biomass is collected and sent for processing at the pyrolysis plant; the second is the use of a pyrolysis klin; the third is when a truck equipped with a pyrolyzed is driven to pyrolyze biomass; the pyrolyzed will be powered by a stream of syngas; and the char will be returned

2.3 CURRENT AND POTENTIAL FUTURE USES OF BIOCHAR

Biochar is used to produce energy in systems because its Sulphur content is minimal, and its burning does not require a NO_x or SO_x reduction method. The ash component of biochar is used as fodder in agriculture; biochar with a low ash content is also used in metallurgy and as an absorbent to eliminate odours from the air and water (Laird, 2009). Biochar is a soil enhancer that stores carbon and creates fertile soils. It reduces nitrogen leaching into ground water, nitrous oxide emission, increases cation-exchange capacity for enhanced soil fertility, soil acid moderation, high water retention rate, and a high number of beneficial soil microbes (2011). These fibers will also be used as geotextiles for the absorption of hazardous spills and as sampling machines for the examination of the contamination of hard surfaces (2010). The first usage of biochar by humans was in cave paintings at the Grotte Chauvet, which date back 38 thousand years and consist of partly burnt wood. In addition, the first biochar use was artistic, with painters using it for painting

during the Renaissance period; the main component of gunpowder was biochar, which was created by alchemists in 9th-century China. The Egyptians used biochar's absorptive properties in wound putrefaction by absorbing putrid gases. In early 20th-century Japan, "Kuntan" biochar was used in rice plantations, ornamental plants, water purification, and the absorption of metallic poisons when magnetite was added to the biochar. Toxic gases on the battlefields of the First World War led to the invention of gas masks using biochar as an absorbent (Meyer, 2009). Use of biochar as a bulking agent for the compositing of chicken manure has been shown by recent research (Use of biochar as a bulking agent for the compositing of poultry manure: Effect on organic matter degradation and humification, 2009). Scientists acknowledge that biochar contributes to the reduction of greenhouse gas emissions, the production of renewable energy, the reduction of waste, the carbon sequestration process, and the amendment of soil that acts as an effective absorbent of agrochemicals (Biochar Application to Soil: Agronomic, Environmental Benefits and Unintended Consequences, 2011). An Assessment of U(VI) removal from groundwater using biochar produced from hydrothermal carbonization An Assessment of U(VI) removal from groundwater using biochar produced from hydrothermal carbonization (2011) found that biochar's physical and chemical properties make it a good absorbent for removing uranium from ground water in an eco-friendly manner. The solid acid catalyst of pyrolyzed biomass is also used to make biochar (Biochar based solid acid catalyst for biodiesel synthesis, 2010). Biochar added to soils to keep earthworm populations high increases the fertility of tropical soils and the sustainability of crop production, as shown by the increase in rice yield (Contrasted effect of biochar and earthworms on rice growth and resource allocation in different soils, 2010). Short-term CO₂ mineralization after additions of biochar and switchgrass to a Typic Kanduitl (2009) found that the addition of biochar to soil increases soil organic carbon concentration, inhibits microbial mineralization, and promotes the organic carbon mineralization of the remains, which aids N immobilization. Biochar is also used in the soil microbial biomass carbon measurement through the fumigation extraction method (Impact of black carbon addition to soil on the determination of soil microbial biomass by fumigation extraction, 2010). Reduced plant absorption of pesticides such as chlorpyrifos and carbofuran with biochar additions to soil (Reduced plant uptake of pesticides with biochar additions to soil, 2009). Biochar derived from the hydrothermal liquefaction of biomass is used to remove lead from water (Removal of lead from water using biochar derived from the hydrothermal liquefaction of biomass, 2009). In plant facilities, biochar-derived bio-oil is used for the large-

scale generation of biohydrogen (Large-scale biohydrogen production from bio-oil, 2010). Biochar and biomass may be used as a biofuel to power boilers, resulting in financial savings, fossil fuel resource conservation, greenhouse gas emission reduction, and employment creation (A review of biomass as a fuel for boilers, 2011). The biochar clumps promote the formation of endomycorrhizal fungi, which reside inside the root cells of plants and whose hyphal mycelium, which resembles root hairs, extends into the soil to collect nutrients for the enhanced growth of plant roots. The agricultural benefits of biochar may be enhanced by combining it with vermiculture, which increases the soil's nutrient availability (Ruehr) (A new magnetic biochar effectively absorbs organic contaminants and phosphate, 2010). Bio-oil produced from the pyrolysis of biomass may be used as a replacement for fossil fuels; it can be refined into biodiesel and gasoline. Biochar is a suitable replacement for coal in the production of energy. Pyrolysis is an effective method for generating electrical energy from biomass, and syngas is used in the manufacturing of methanol and hydrogen. In addition, bio-oil is composed of organic acids that corrode steel containers and include biochar that damages truck injectors (2008). (Sorption and ecotoxicity of pentachlorophenol-contaminated sediment modified with biochar derived from rice straw, 2010). Biochar generated from rice straw is used for the adsorption of pentachlorophenol, an organic pollutant, from sediments as well as measuring the adsorption capacity. Biochar applied to soils with coconut fibre tuff potting medium induces systemic resistance to fungal pathogens such as powdery mildew, grey mould, and broad mite on tomato and pepper, which contain the diseases in their leaf parts (Induction of Systemic Resistance in Plants by Biochar, a Soil-Applied Carbon Sequestering Agent, 2010). Biochar is also used to modify sand-based turfgrass root zones, where it lowers saturated hydraulic conductivity, reduces rooting depth, and enhances soil water retention in sand for plants in sand-based root zones (Brockhoff, 2010). Biochar influences nitrogen, phosphorus, and Sulphur changes in the soil ecosystem; the biochar mechanism modifies the transformation of soil nutrients (DeLuca et al., 2009). Pecan-based biochar that is not activated with ground switchgrass (*Panicum virgatum*) is utilized to increase the soil carbon content, infiltration, aggregation, and water-holding capacity of Norfolk Loamy Sandy soils with poor physical properties and low soil carbon content (Influence of Pecan Biochar on Physical Properties of a Norfolk Loamy Sand, 2010). Biochar electrodes will replace activated carbon electrodes for supercapacitor-like energy storage (Topre, 2011). When biochar generated from sawdust by rapid pyrolysis at 500 degrees Celsius is put on sandy loam soil, low amounts of atrazine pesticide are

absorbed (Mesa, 2006). Biochar derived from the thermal decomposition of specific biomass can be used as a renewable fuel in a power plant; pyrolysis is used in developing countries to improve efficiency, sustainability, and biomass reduction; and the pyrolysis biochar process controls greenhouse gas emissions. Pyrolysis is advantageous for the reduction of trash destined for landfill disposal (Brownsort P.A., 2009). Biochar is used to counteract the detrimental consequences of forest biomass clearance; biochar generated from hardwood has carbonate concentrations that reduce soil acidity, reduce aluminium saturation, and enhance base saturation. The addition of biochar to soils with a high pH may lead to nutritional deficits in plants and crops. (Coleman, 2009).

2.4 EXPLANATION OF MAGNETIC BIOCHAR

Magnetic biochar is a charcoal that is produced by the synthetic mixing of powdered biomass with magnetite or iron oxide, followed by pyrolysis at varying temperatures to produce a mixture of biochar and magnetite or iron oxide. Magnetic biochar is becoming increasingly intriguing because it is a multifunctional substance with environmental applications such as carbon storage capacity, greenhouse gas reduction, and a material that absorbs metallic toxins and pollutants, as well as agricultural applications such as soil fertility improvement, increased plant growth, soil nutrient improvement, enhanced soil performance, and increased soil cation exchange capacity. Biochar derived from plant waste and animal residue has been used for organic pollutant adsorption, while biochar derived from animal manure has been used to adsorb both organic and metallic contaminants. High-temperature biochar has a higher absorption capacity than low-temperature biochar due to its larger surface area of aromatic compounds and high microporosity. At the current level of magnetic biochar research, biomass is synthetically combined with a magnetic chemical solution or magnetite in a pyrolysis machine at varying temperatures. Baoling Chen, Zaiming Chen, and Shaofang Lv of China's Zhejiang University formulated a magnetic biochar for extracting hydrophobic organic compounds and phosphate from wastewater. Magnetic biochar is a cost-effective absorptive material that has garnered increased interest in recent years due to its advantages and uses. Heavy metals and organic poisons in water are held together by biochar made from agricultural waste. Also, the use of magnetic biochar to remove metal toxins from polluted soils is still being

researched, as is the sorption experiment that shows how magnetic biochar adsorbs metal toxins when applied to soil (Removal of Phosphate from aqueous solutions by biochar derived from anaerobically digested sugar beet tailings, 2011). Attractive magnetic microstructures are created by combining the skeletal structure of a leaf with iron acetate in a vacuum, removing any excess liquid, drying the mixture in warm air or an oven, and pyrolyzing it at 700 degrees Celsius with nitrogen to drive out the air, at which point the skeletal structure turns black, becomes strongly magnetic, and is attracted to a magnet (Bio templating of Metal Carbide Microstructures: The Magnetic Leaf, 2010). X-ray diffraction, BET surface area measurement, and scanning electron microscopy were utilized to characterize the magnetic absorbent's forms and characteristics. Environmental technology, analytical chemistry, and mining all use magnetic separation technology for the effective separation of magnetic materials. The advantage of this technology is that it can treat a large quantity of wastewater in a short amount of time without producing any pollution. Magnetic biochar is typically composed of magnetic nanoparticles, and recent research has been conducted on the synthesis of magnetic-chitosan matter as an absorbent for fluoride removal and an Arabic gum magnetic absorbent, which is used for the removal of copper ions. The incorporation of magnetic characteristics into biomass to produce biochar would increase its ability to absorb metallic poisons (Removal of cationic dyes from aqueous solution utilizing magnetic multi-wall carbon nanotube nanocomposite as an adsorbent, 2009). For removing heavy metals, hydrocarbons, and nitrates from soil and water, absorbent-based biomass is a cost-effective and environmentally beneficial method. Effect of particle size on phosphate adsorption in bio sorbents made from wood particles treated with anionic polymer and iron salt (2008; Bio sorbents made from wood particles treated with anionic polymer and iron salt: Effect of particle size on phosphate adsorption).

The capacity of organic arsenate and monomethyl arsonate absorption by calcium-made magnetic biochar was tested (Organic arsenic adsorption onto a magnetic sorbent, 2009). Through a chemical co-precipitation process, biomass is combined with powdered copper iron (II) oxide to produce magnetic biochar. This biochar is then used to absorb acid orange II in water and is separated from the medium by a magnetic process (CuFe₂O₄/activated carbon composite: a novel magnetic adsorbent for the removal of acid orange II and catalytic regeneration, 2007). Magnetic biochar has many applications in the magnetic invention of energized carbon made by the

combination of magnetite and charcoal. Magnetic biochar is also created when iron (II) sulphate heptahydrate is mixed and dissolved in water about one hundred centimeters cubed, mixed with powdered activated carbon, and sodium hydroxide is added dropwise over the course of five minutes so that hydrated iron oxides precipitate (Safarik, 1996). Copper, Zinc, and Cadmium are extracted from soils using an absorbent containing iron filings and magnetic separation to collect the filings (Heavy Metal Removal from Soils Utilizing Magnetic Separation: 1. Laboratory Experiments, 2007). Magnetic biochar, an absorbent developed and used for heavy metal ion removal, relies on the interaction of specific compounds with operative groups found on the absorbent surface, with the operative groups determining the capacity, effectiveness, selectivity, and reusability of the absorbent. According to a recent study, magnetic biochar made from magnetite in combination with amino groups was developed for the absorption of cations. The magnetic separation method is beneficial to the environment because it does not produce contaminants, particularly magnetic biochar, which is composed of magnetite particles with Organo silane or polymer on the surface of the absorbent (Application of bifunctional magnetic adsorbent to adsorb metal cations and anionic dyes, 2010). magnetic dendritic materials for amazingly effective adsorption of dyes and drugs (2010). The chemical CuFe_2O_4 is recovered using a magnetic separation method from magnetic biochar, which is an absorbent composed of Cu (II) and Fe (III) oxides used to remove arsenic. characterization and analysis of the arsenic absorption characteristic of magnetic biochar (Arsenic absorption by magnetic adsorbent CuFe_2O_4 , 2003). Magnetic modified organic matter containing magnetic particles has gained a great deal of attention due to its ability as a magnetic absorbent for organic and inorganic compounds, which has been successfully applied in the separation of xenobiotics, nucleic acids, and proteins. This is interesting because it is used for the removal of heavy metals from waste (i.e., aqueous), alternative methods to gravitational and filtration processes, and manipulation of magnetism with magnetic biochar (Mosiniewicz-Szablewska, 2010).

3.0 METHODOLOGY

3.1 EXPERIMENTAL PROCEDURE

Doctor Chris Ennis of the Clean Environment Management Centre (CLEMANCE), School of Science and Engineering, Teesside University, Middlesbrough, United Kingdom, provided SRC Willow with a grain size of less than 2 mm (about 0.08 in) as the raw biomass material; 20.25 grammes of iron (III) chloride and 15.91 grammes of iron (II) chloride in solute form were used to make standard and reagent solutions of 1.0M and 0.1M, respectively. In addition, ultraviolet-visible spectroscopy was conducted on standard solutions of 0.05M, 0.1M, 0.2M, and 0.4M iron (II) chloride and iron (III) chloride, using 460 nm as the spectrum measuring wavelength using the JASCO V-630 Spectrophotometer. The pH suspension was adjusted to 10, as indicated by universal indicator paper, and stirred for 30 minutes. Consequently, the 1.0 M iron solution combination with SRC willow and the 0.1 M iron solution mixture with SRC willow were filtered to separate the deposits. The deposits from the 1.0M and 0.1M iron solution SRC willow mixtures were oven-dried for two days at 105 degrees Celsius, weighed, and placed in ceramic boats for pyrolyzing in the Carbolite electric tube furnace, which began at 10:15 am and lasted one day; the temperature was lowered to thirty degrees Celsius when it reached 400 degrees Celsius. After that, the 1.0 M magnetic charcoal and 0.1 M magnetic charcoal residues were weighed and placed in sample containers that have been labelled. Copper sulphate solutions of 2 solutions of 20ppm, 40ppm, 60ppm, 80ppm, 100ppm and 200ppm were subjected to atomic absorption and ultra-violet visible spectrometry analysis, including spectrum measurement and fixed wavelength measurement at 300nm. 40ppm was used for 1.0 M iron solution magnetic biochar; 60ppm and 3ppm will be mixed with 1.0 M, 0.1 M iron solution magnetic biochar, and activated charcoal lively.



Fig 1 SRC willow



Fig 2 Carbolite Electric Tube



Fig 3 1.0 M iron (II) chloride standard solution



Fig 4 1.0 M iron (III) chloride standard solution



Fig 5 0.1 M iron (II) chloride standard solution



Fig 6 0.1 M iron (III) chloride standard solution



Fig 7 Weighing of iron (II) chloride and iron (III) chloride solutes



Fig 8 Filtering process of 1.0 M iron solution SRC willow



Fig 9 Dried 1.0 M iron solution SRC willow



Fig 10 Dried 0.1 M iron solution SRC willow



Fig 11 1.0 M magnetic biochar made at 400 degrees Celsius



Fig 12 0.1 M magnetic biochar made at 400 degrees Celsius

3.2 SAMPLES CHARACTERISATION

The most popular infrared spectroscopy is Fourier transform infrared spectroscopy, in which infrared light travels through a sample and is both absorbed and transmitted. The spectrum illustrates the molecular absorption and transmission, which determine the sample's molecular footprint. Since no two molecules with identical structures can have identical infrared spectra, infrared spectrometry is particularly helpful and often required for many sorts of analyses. FTIR may be used for the identification of unknown substances, the evaluation of sample consistency and quality, and the quantification of mixture components. An infrared spectrum illustrates a sample's imprint in which the absorption peaks correspond to the vibration frequencies between the atomic bonds that comprise the material. Infrared spectroscopy may provide conclusive identification and is an excellent quantitative analytical method. FTIR spectroscopy is a very multiplexing process in which all optical frequencies from their origin are observed over a given period known as the scan time; the resultant digital signal generated from an infrared light passing through a sample is known as the interferogram, which depicts the intensities in the sample. The peak height of FTIR spectroscopy represents the absorbance values on a scale set by Beer's equation, which stipulates that concentration is directly proportional to absorbance, as

demonstrated by: $C = A/a \cdot b$; C is absorptivity and b is the sample's pathlength. A sample absorption or transmission spectrum is determined by the logarithmic ratio of a sample single-beam spectrum to a background single-beam spectrum. The single beam spectrum is the measurement of the intensity of infrared light that reaches the detector when a sample is placed in the infrared light path, whereas the background single beam spectrum is the measurement of the intensity of infrared light that reaches the detector when a sample is not placed in the path of infrared light; the chemical constituents of the sample determine the frequencies and absorption bands (E, et al.). Fourier transform infrared spectroscopy is used to identify 1.0 M and 0.1 M iron solution magnetic biochar to determine its functional groups; during infrared spectrometry, infrared radiation is passed through the magnetic biochar, with some of the radiation being absorbed and the rest being transmitted. Laser radiation is a spectrum composed of transmittance and absorption; the study assesses the quality and uniformity of magnetic biochar (2005). Using a Perkin Elmer Spectrum 100-FTIR spectrometer, Fourier transform infrared spectra were acquired in the 4000-530 cm^{-1} (about 17.39 μm)-1 range for 1.0 M and 0.1 M iron solution magnetic biochar.

Electron microscopy is defined as a science that requires the electron microscope as a device that uses a beam of electrons to create an image of a sample. Electron microscopy operates in a vacuum and the electron beams are focused and the images are magnified with the aid of electromagnetic lenses. Electron microscopy employs a much shorter wavelength and reduced resolution when the accelerating voltage is increased, and when the electron velocity is increased, which results in a lower resolution. There are two sorts of electron microscopes: the scanning electron microscope used for this project and the transmission electron microscope. In the late 1930s, Manfred von Ardenne invented the scanning electron microscope, which uses secondary electrons to create a three-dimensional image. The scanning electron microscope can magnify samples between ten and a hundred thousand times and has an extremely high magnification range of more than two hundred thousand, allowing the electron microscope to view samples in much greater detail (Stadtlander, 2007). Using a Hitachi S-3400N scanning electron microscope with an accelerating voltage of 15 keV and a magnification of X900, the electron image, spectra micrograph, and the number of elements in terms of weight in percentage were captured for magnetic biochar from 1.0 M and 0.1 M iron solutions. In most crystalline solids, X-rays have the same wavelength as the atomic arrangement and spacing. Bragg's law states that x-rays will interfere constructively and form a high-intensity spot on film when x-rays scattered from

planes have path differences distinguished by several wavelengths. The extra path length is $2d\sin\theta = n\lambda$ where λ is the wavelength, n is the integer order of the reflection, and d is the distance between lattice planes. This is not comparable to the normal angle of incidence in optics but is comparable to the angle of incidence in the lattice plane (2010). The anatomy of X-ray diffraction consists of the intensity of the diffraction signal plotted against the diffraction angle; θ and d (nm) may also be used; the most common wavelength used in X-ray diffraction is 1.54 (Cu K); and the signals in the diffractogram are referred to as Bragg peaks, which depict the peak position, peak height, peak area, and peak width. For precise analysis of X-ray diffraction data requires the separation of the signal of the sample from the background and noise; for improvement of the signal/noise ratio, the intensity of the incoming beam from the synchrotron source must be increased; the wavelength of the sample beam must be shortened; the amount of sample beam must be increased. To determine any crystalline structure in the 1.0 M iron solution magnetic biochar, X-ray diffraction patterns were recorded on an X-ray diffractometer equipped with Cu K radiation with a wavelength of 1.5418 or Mo K radiation with a wavelength of 0.71073 across the 2 θ -range of 20–80°. The X-ray Diffraction experiment consists of two sections: the powder technique and the Laue method. The powder method is used to identify unknown samples. The orientation of a single crystal of unknown material is determined using a Laue camera; the powder approach produces X-rays when Bremsstrahlung radiation is formed when energetic electrons strike a Cu target; the more energetic the incoming electrons, the wider the X-ray band produced. To isolate the K α line, a filter is utilized; the monochromatic beam scatters off the randomly oriented powder crystallites, causing the diffraction peak to increase at detector angles of 2θ per Bragg's law. For the Laue technique, a continuous band of white X-rays is utilized to produce diffraction spots on 2D film wherever the incident, scattered wave vectors are sufficient for the procedure. The Laue technique assists in limiting incoming x-rays via the utilization of wavelengths. UV/VIS Spectroscopy utilizes the ultraviolet and visible ranges of electromagnetic radiation and is also known as Electronic Spectroscopy. It demonstrates that high-energy photons disrupt the electron distribution of a molecule, and the absorption intensity is calculated by the molar extinction coefficient (ϵ), which is defined in terms of incident light intensity (I_0), transmitted light intensity (I), solution concentration (c), and path length (l). When it is larger, the probability of absorption increases (UVV11). The molar extinction coefficients for distinct compounds are unique, allowing the UV/VIS spectroscopy of an unidentified chemical to be determined. UV/VIS spectroscopy is

used to determine the wavelength and maximum absorbance of substances. According to Beer's law, absorbance is directly proportional to concentration and route length (Ult11). using light with wavelengths ranging from 400 to 780 nanometers, which corresponds to the area of energy space where molecules undergo an electronic transition (F, et al.). Ultraviolet infrared spectrometry was performed on the copper solution mixture extracted from 10mg (about the weight of a grain of table salt) of 1.0 M iron solution magnetic biochar mixed in 1ml (about 0.03 oz) of 40ppm copper standard solution and the extracted deionized water mixture from 10mg (about the weight of a grain of table salt) of 1.0 M iron solution After roller mixing for 24 hours, the magnetic biochar was mixed in 1ml (about 0.03 oz) of deionized water and 1ml (about 0.03 oz) of deionized water, and the copper solution mixture was extracted from 30mg (about the weight of a grain of rice) of 1.0 M iron. Atomic absorption spectrometry is a technique used for elemental analysis of samples; determining the concentration of an element in a solution using a light source that emits a specific wavelength of light that atoms will absorb. The amount of energy absorbed at a specific wavelength is directly proportional to the number of atoms of a particular element. A hollow cathode lamp and an electrodeless discharge lamp are two common light sources used in atomic absorption spectrometry. The atomizer prepares atoms of ground stag state for atomic absorption spectrometry by applying thermal energy to break the bonds that hold atoms together. A monochromator is used to hide the light of a specific wavelength that is used, and a detector is used to measure light precisely (M, et al., 2008). AAS can be used to test wastewater, animal feed, soil, and lubricating oil additives. It can also be used in clinical analysis. mic absorption spectrometry is the measurement of the amount of energy absorbed by a sample using a detector to measure the wavelengths of light transmitted and a signal processor to integrate the wavelength variations. It is an elemental analysis process used for the analysis of samples from the chemical, food, metal, and pharmaceutical industries; it is the process of checking the sensitivity of atomic absorption spectroscopy, determining the amount of copper in the copper standard solution, and generating a calibration curve; the graph of absorbance versus concentration is plotted on a Microsoft Excel sheet to demonstrate Beer's-Lambert law; and the atomic absorption spectroscopy process consists of two steps. Also, the amount of a known element in a sample can be found by making a calibration curve. In this method, a known wavelength is chosen, and the detector only measures the energy emitted at that wavelength. As the concentration of the sample goes up, the amount of energy absorbed by the sample goes up in direct proportion. A calibration curve is

drawn from the points, and the substance's concentration can be figured out from its absorbance. The typical concentration is the analyte concentration that produces an absorbance of 0.0044, and it is important for evaluating the performance of the AAS instrument since a low concentration value suggests more sensitivity (Abubakar, 2010). Copper standard solutions of 1 ppm, 2 ppm, and 4 ppm were subjected to atomic absorption spectrometry. These solutions were derived from 20ppm of standard solution, which was produced by weighing 0.1966g of blue copper (II) sulphate pentahydrate. Using an ICE 3000 C113300102 V1.30 Atomic Absorption Spectrophotometer, the concentration and signal absorbance of three copper standard solutions were measured. Iron (II) chloride, which is used to make biochar magnetic, is a paramagnetic solid with a pale green color, a molar mass of 198.81 g/mol, a density of 1.39g/cm³, melting and boiling points of 105 and 1023 degrees Celsius, respectively, and solubility in water at 100 degrees Celsius of 105.7g/100ml (about 3.38 oz) of water. In addition, the iron (III) chloride utilized is purple red in transmitted light and becomes yellow when 6 moles of water are added. It has a molar mass of 270g/mol, melting and boiling temperatures of 37 and 280 degrees Celsius, and a solubility in water of 92g/100ml (about 3.38 oz) of water at 20 degrees Celsius. Sodium hydroxide is the caustic metallic base used as a pH regulator (i.e., increasing the alkalinity of a mixture) when mixed and stirred with SRC willow with iron (II) and iron (III) chloride. Sodium hydroxide has a molecular mass of 39.9 g/mol, a density of 2.13 gm 3, melting and boiling points of 318 and 1388 degrees Celsius, respectively, and a solubility in water of 0.05%.



Fig 13 FTIR Spectrometry on magnetic biochar



Fig 14 Hitachi S-3400N Scanning Electron Microscope

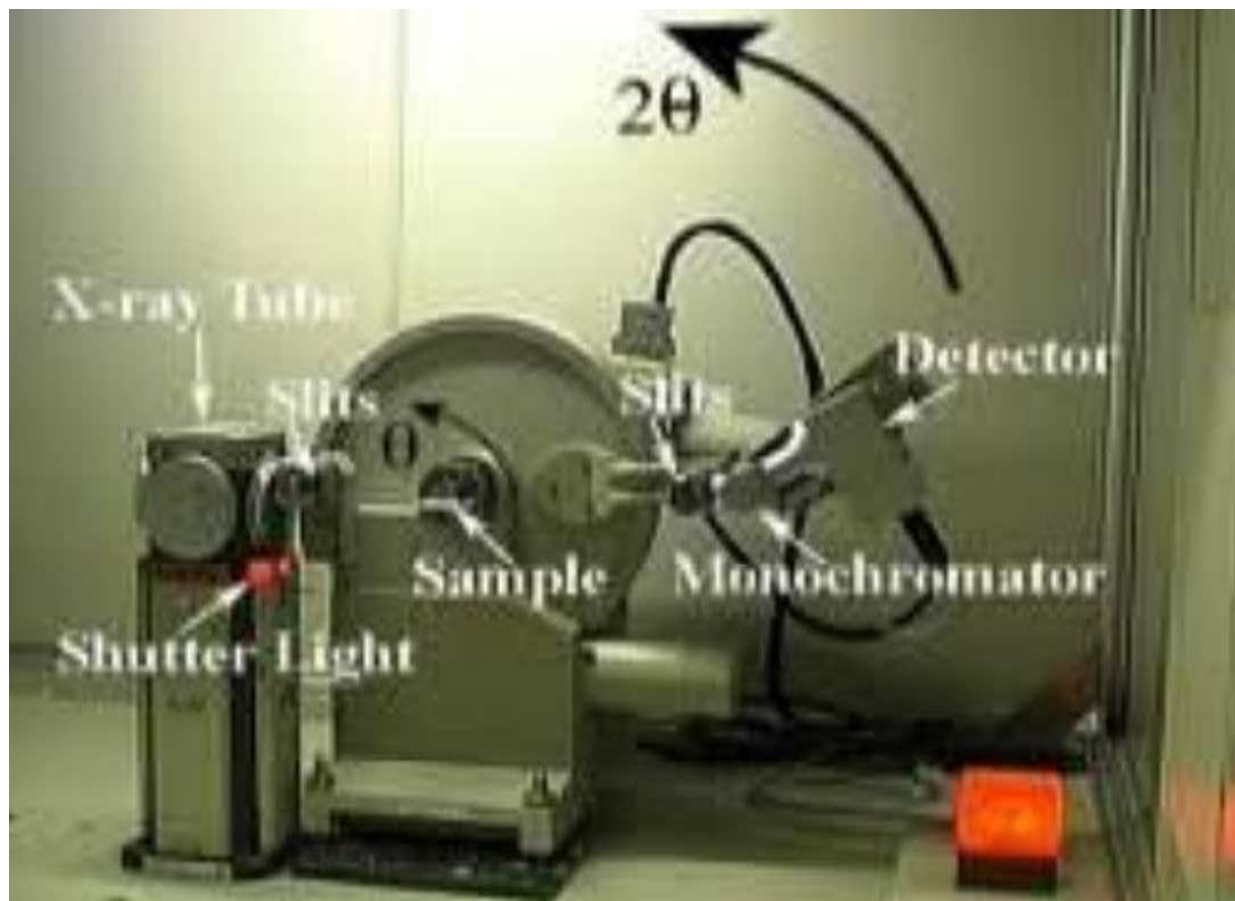


Fig 15 Schematic Diagram of X-ray Diffractor

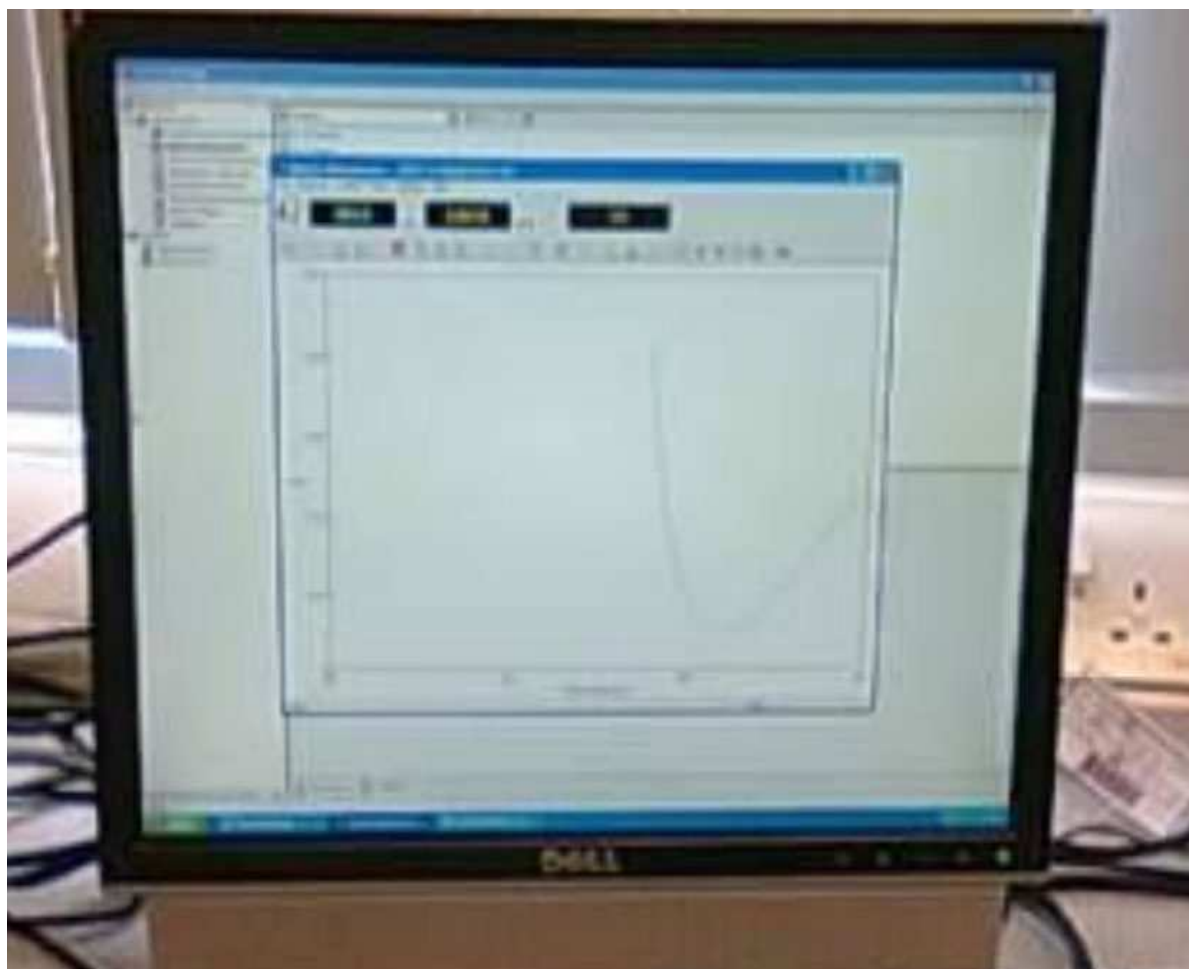


Fig 16 U V/VIS Spectrometry digital graph of iron solutions



Fig 17 Electron image of magnetic biochar

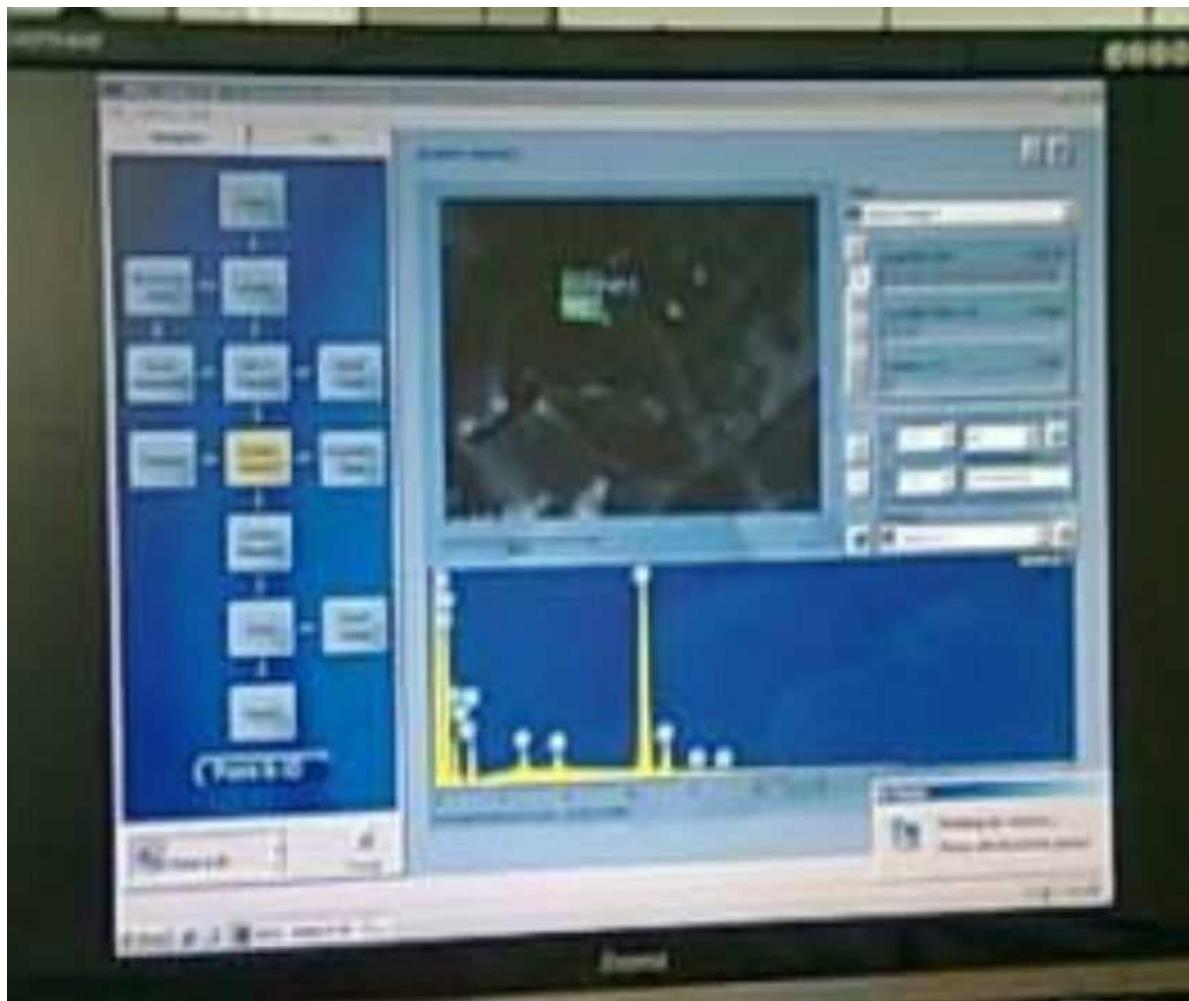


Fig 18 Scanning Electron Microscopy analysis of magnetic biochar



Fig 19 Concentrations of iron (II) chloride standard solutions



Fig 20 Concentrations of iron (III) chloride standard solutions



Fig 21 Filtering of activated charcoal from 1ml (about 0.03 oz) of deionized water



Fig 22 Three samples on a Stuart roller mixer machine



Fig 23 Sixteen samples on a Stuart roller mixer machine



Fig 24 Atomic absorption spectrometry of sixteen samples



Fig 25 JASCO V-630 U V/VIS Spectrophotometer

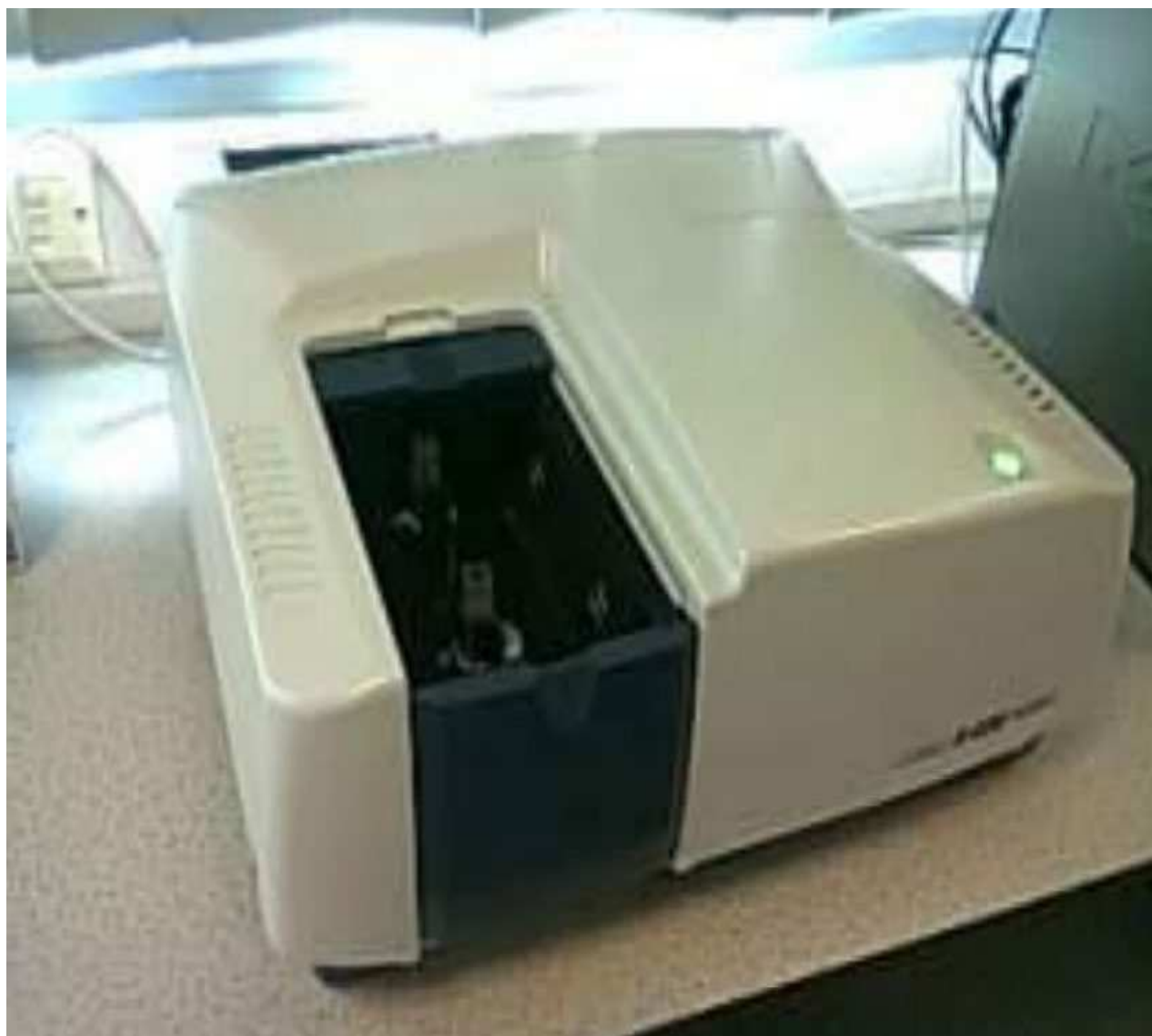


Fig 26 JASCO V-630 U V/VIS Spectrophotometer with cuvettes

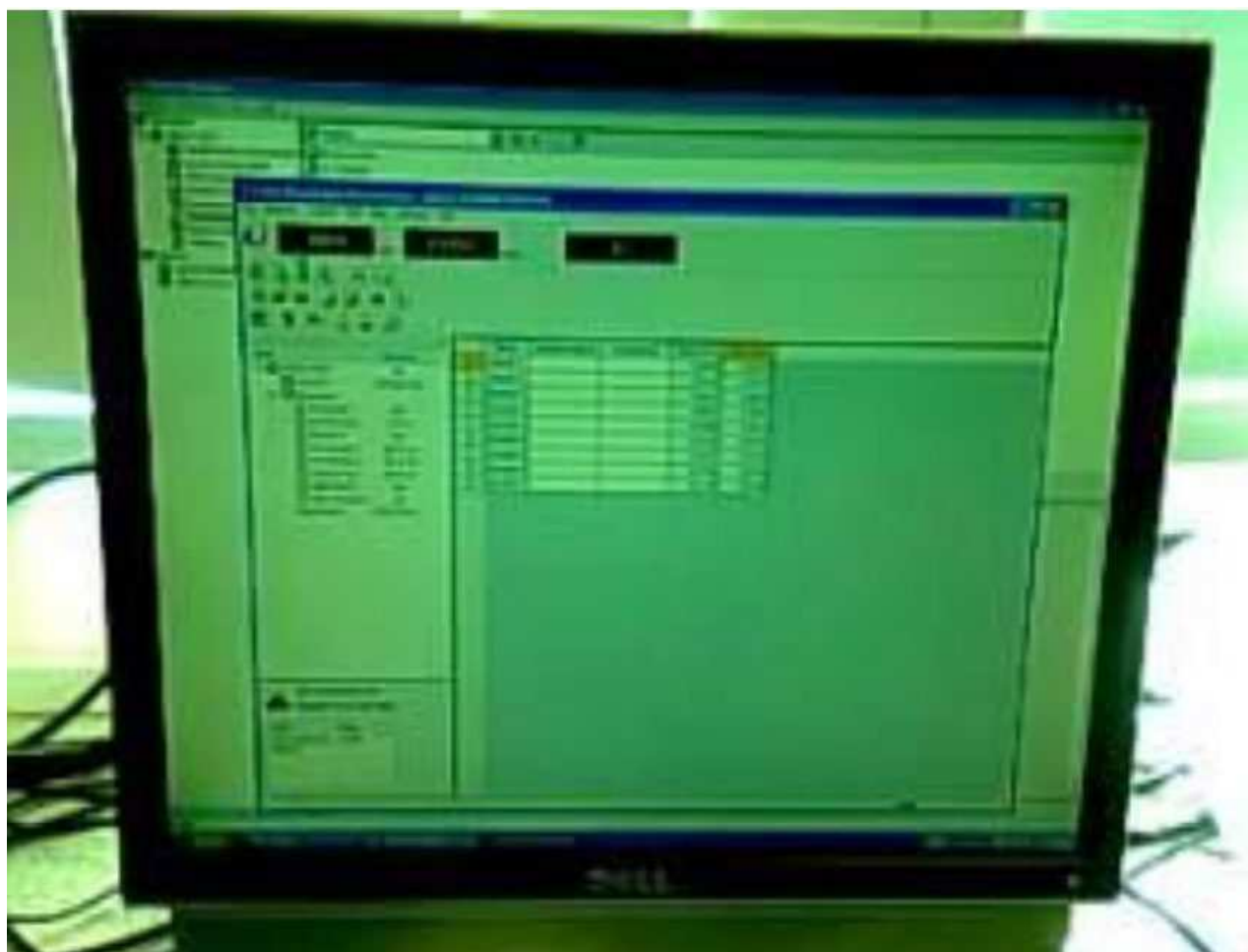


Fig 27 Fixed wavelength readings for concentrations of copper solutions

3.2 ADSORPTION EXPERIMENT

Sodium copper sulphate pentahydrate solution in 2% nitric acid was chosen as a model compound due to its molecular mass, density, solubility in water, melting point, and standard molar entropy of 249.70g/mol, 2.284g/cm³, 316g/l (0o c), 150o c (-5H₂O), and 109JK¹mol⁻¹. This compound can be used as an herbicide, fungicide, or pesticide. 10mg (about the weight of a grain of table salt) of 1.0 M iron solution magnetic biochar is weighed by difference on a weighing machine and put in a sample tube with 1ml (about 0.03 oz) of deionized water, followed by 10mg (about the weight of a grain of table salt) of 1.0 M iron solution magnetic biochar in 1ml (about 0.03 oz) of 40ppm copper standard solution and 1ml (about 0.03 oz) of deionized water. All sample tubes are labelled and put for 24 hours in a Stuart roller mixer. Also, three samples of 30mg (about the weight of a grain of rice) of 1.0 M iron solution magnetic biochar were weighed by difference and mixed with 1ml (about 0.03 oz) of 60ppm copper standard solution for each sample; one sample tube of 30mg (about the weight of a grain of rice) of 1.0 M iron solution magnetic biochar was mixed with 1ml (about 0.03 oz) of deionized water; three sample tubes of 20mg (about twice the weight of a grain of table salt) of 0.1 M iron solution magnetic biochar were mixed with 1ml (about 0.03 oz) of 60ppm copper standard solution for each sample tube, and one sample tube of 20mg (about twice the weight of a grain of table salt) of 0.1 M iron solution magnetic biochar was mixed with 1ml (about 0.03 oz) of deionized water. All sample tubes are labelled and put for 72 hours (about 3 days) in a Stuart roller mixer. The 1.0 M and 0.1 M iron magnetic biochar solutions were separated from the solids by inserting a magnet at the bottom of sample tubes containing magnetic charcoal and sucking out the liquids with a 1 ml (about 0.03 oz) rubber pipette; the solutions from activated charcoal were separated by filtering. The concentration of the liquids extracted from the nineteen sample tubes was evaluated using the JASCO V-630 U V/VIS spectrophotometer to obtain multiple readings of spectra measurements and a fixed wavelength measurement at 300nm for each liquid extracted from the solids. In addition, a 3ppm standard solution of copper was prepared, and three samples of 3mg of 1.0 M iron solution magnetic biochar were weighed by difference and mixed with 1ml (about 0.03 oz) of 3ppm of copper standard solution each for the samples; 3mg of 1.0 M iron solution magnetic biochar mixed with 1ml (about 0.03 oz) of deionized water; and three sample tubes of 2mg of 0.1 M iron solution magnetic biochar each was mixed with 1ml (about 0.03 oz) of 3ppm of copper standard solution for each sample. The sample tubes are labelled and mixed for 72 hours (about 3 days) in a Stuart roller mixer. In addition, the 1.0 M

and 0.1 M iron solution magnetic biochar solutions were separated from the solid particles of magnetic biochar by placing a magnet at the bottom of the sample tubes and sucking the solutions with a 1 ml (about 0.03 oz) rubber pipette; the solution from activated charcoal was separated via filtration. The signal absorbance and concentration of liquids extracted from sixteen sample tubes were evaluated using the atomic absorption spectroscopy ICE 3300102 V1.30 at a fixed wavelength of 324.8nm; the atomic absorption spectrometer's typical concentration value was 0.0469. A calibration graph is a line formed from points when the absorbance of metallic solutions such as iron (II) chloride, iron (III) chloride, and copper (II) sulphate pentahydrate is measured with a spectrophotometer and plotted with various concentrations prepared; when plotted, there is a linear relationship between the concentration of iron (II) chloride ions, iron (III) chloride ions, and copper (II) sulphate pentahydrate. At given wavelengths of 460nm and 300nm, solutions with low concentrations of iron (II) chloride, iron (III) chloride, and copper (II) sulphate pentahydrate have low absorbance values, while solutions with high concentrations of iron (II) chloride The calibration equation is the trendline equation that is fitted into the calibration, with the slope of the resultant line representing the molecular absorptivity of the solution (i.e., $y=mx+c$).



Fig 28 2000ppm of copper (II) sulphate pentahydrate in 2% nitric acid

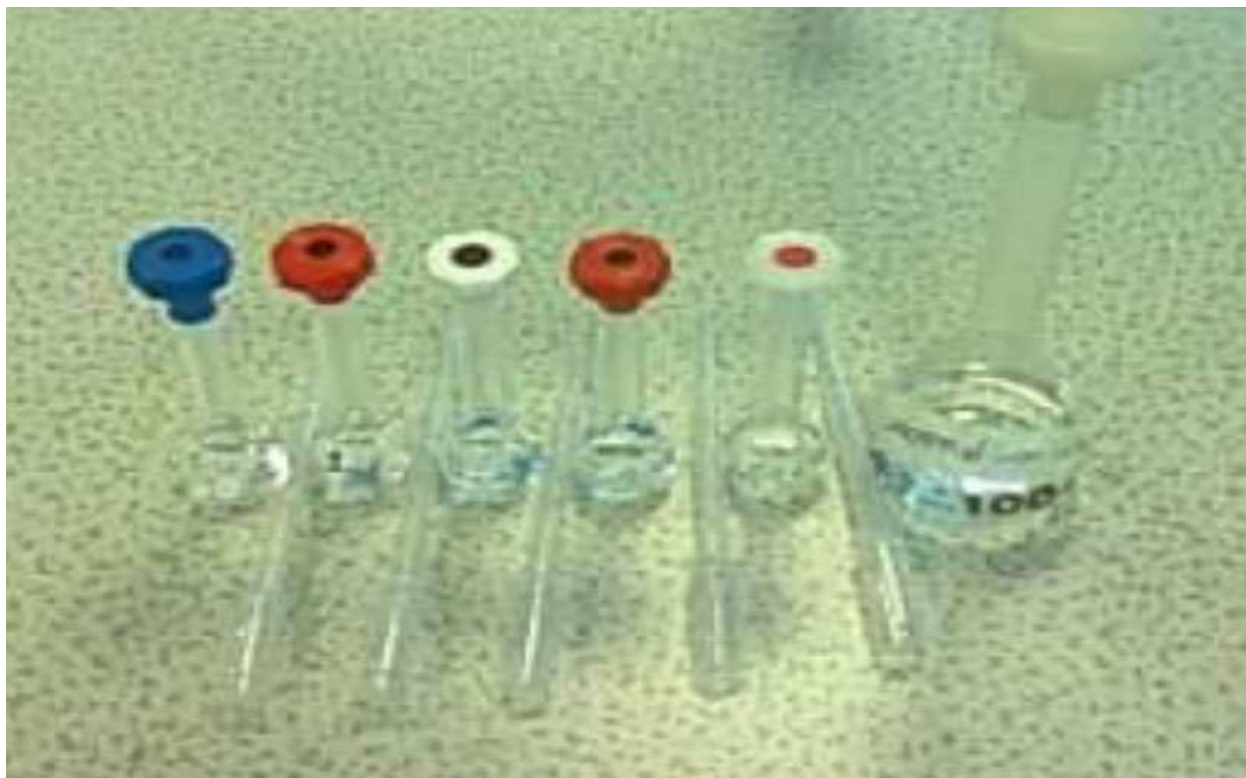


Fig 29 the six concentrations of copper sulphate standard solutions with 1ml (about 0.03 oz) rubber pipettes



Fig 30 a canister of 5M sodium hydroxide

4.0 RESULTS AND DISCUSSION

4.1 CHARACTERISATION OF SAMPLES

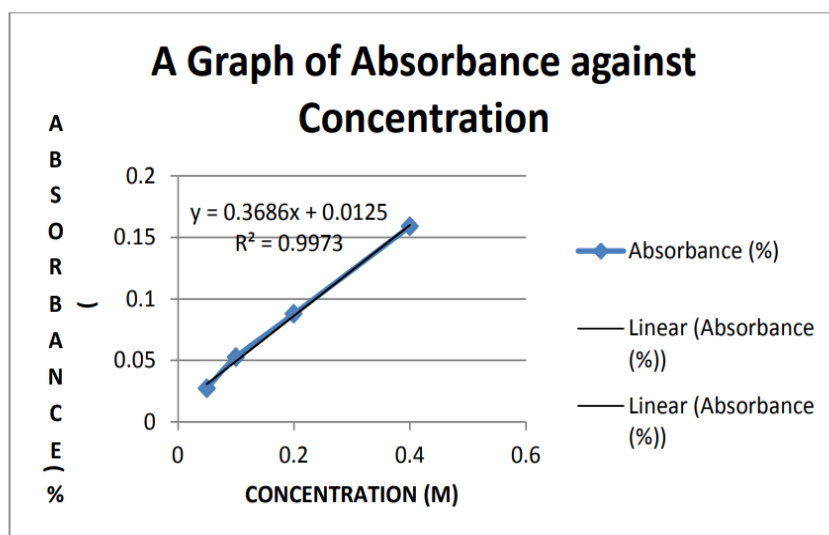
After pyrolysis at 400 degrees Celsius in a Carbolite electric tube furnace, the weight of 1.0M and 0.1M iron solution magnetic biochar is 1.1996g and 0.1571g, respectively. The U V/VIS Spectrometry study of 0.05M, 0.1M, 0.2M, and 0.4M iron (II) chloride standard solutions reveals absorbance values of 0.0273159, 0.0525201, 0.0877593, and 0.158808%, respectively. The slope of the graph is 0.3686 and the R-squared value is 0.09973; for iron (III) chloride standard solutions of 0.05M, 0.1M, 0.2M, and 0.4M, the signal absorbance values are 0.144641, 0.289280, 0.568550, and 1.157115%, respectively. The slope of the graph is 2,891 and the R-squared value is 0.9999. The calibration curve was created using a Microsoft Excel sheet. The absorbance values of 20ppm, 40ppm, 60ppm, 80ppm, 100ppm and 200ppm of copper standard solutions were obtained from repeated spectra measurement readings at wavelengths between 255-350nm and repeated fixed wavelength readings at a wavelength of 300nm using a U V/VIS Spectrophotometer with calibration graphs, displaying R-squared values and equations of the graphs depicted in Table 3, Graph 3, Graph 4, Graph 5, and Graph 5. In addition, U V/VIS Spectrometry for 10mg (about the weight of a grain of table salt) of 1.0 M iron solution magnetic biochar with 1ml (about 0.03 oz) of deionized water, 10mg (about the weight of a grain of table salt) of 1.0 M iron solution magnetic biochar with 1ml (about 0.03 oz) of 40ppm copper standard solution and 1ml (about 0.03 oz) of deionized water only, with absorbance values for spectra measurement repeated readings at wavelengths of 220-350nm and fixed wavelength measurement repeated readings at 300nm with a blank reading of 0.3693 are The liquids extracted from the sixteen samples, which consist of 1.0 M iron solution magnetic biochar, 60 ppm copper standard solution, deionized water, 0.1 M iron solution magnetic biochar, and activated charcoal, are placed in the U V/VIS Spectrophotometer, and the absorbance values are displayed below. When dried, the 0.1 M and 1.0 M iron standard solutions including biomass (SRC Willow) weigh 0.3324 g and 8.9660 g, respectively. According to Fourier transform infrared spectrometry analysis of 1.0 M and 0.1 M iron solution magnetic biochar, the peaks at 519.15 cm^{-1} , 530.46 cm^{-1} , 556.32 cm^{-1} and 584.10 cm^{-1} for the 1.0 M magnetic biochar are attributed to Fe-O, and it demonstrates that 1.0 M iron (II) chloride and iron (III) chloride were introduced into the

biochar. In addition, peaks seen at 1172.23 cm^{-1} and 3789.37 cm^{-1} indicate the existence of C-O-C and OH functional groups, respectively. The peak values of 0.1 M iron solution magnetic biochar at 1428.33 cm^{-1} and 2189.50 cm^{-1} indicate the CH₂ group; both magnetic biochar's are pyrolyzed at 400 degrees Celsius, and 1.0 M iron solution magnetic biochar contains one-tenth more iron (II) and iron (III) chloride than 0.1 M iron solution magnetic biochar. The results of the X-ray diffraction analysis of the 1.0 M iron solution magnetic biochar are depicted in Graph 12; peak positions at 30.06 degrees, 31.76 degrees, 35.56 degrees, 43.1 degrees, 45.5 degrees, 53.28 degrees, and 62.64 degrees display peak heights with maximum intensities of 118 counts, 360 counts, 323 counts, 84 counts, 193 counts, 41 counts, 92 counts, and 140 counts, respectively. Also, the 1.0 M iron solution magnetic biochar was composed of phases of iron chloride constituents and biochar. But x-ray diffraction analysis was not done on the magnetic biochar from the 0.1 M iron solution because it does not have a lot of iron (II) chloride and iron (III) chloride. Scanning electron microscopy analysis of 1.0 M iron solution magnetic biochar pyrolyzed at 400 degrees depicts a high percentage of iron oxide in terms of weight, atomic composition, and compound composition; oxygen has a high percentage of both atomic composition and weight; chloride has a higher percentage in terms of weight than sodium oxide, but sodium oxide has a higher percentage in terms of atomic composition. For the 0.1 M iron solution, magnetic biochar in terms of weight, atomic and compound composition, pyrolyzed at 400 degrees shows a high percentage of iron oxide; following sodium oxide, chloride has a higher percentage of weight than calcium oxide; calcium oxide has a lower percentage of atomic composition than chloride; and calcium oxide has a higher percentage of compound composition than chloride. Sodium oxide composition is greater in 0.1 M iron solution magnetic biochar than in 1.0 M iron solution magnetic biochar, chloride composition is greater in 1.0 M iron solution magnetic biochar than in 0.1 M iron solution magnetic biochar, calcium oxide is present in 0.1 M iron solution magnetic biochar but not in 1.0 M iron solution magnetic biochar, and iron oxide composition is greater in 1.0 M iron solution magnetic biochar than in 0.1 M iron solution magnetic biochar. Atomic absorption spectroscopy was performed on copper standard solutions of 1ppm, 2ppm, and 4ppm, which were prepared from a 20ppm of copper solution that was prepared from a 1000ppm copper solution with 2% nitric acid by calculating and weighing 0.1966g of copper from copper sulphate pentahydrate on an Explorer Pro weighing machine; the signal absorbance for the copper solutions is 0.131%A,

0.212%A, and 0.425%A Below are the signal absorbance and concentration data for the sixteen samples consisting of 1.0 M iron solution magnetic biochar, 0.1 M iron solution magnetic biochar, 60 ppm of copper standard solution, deionized water alone, and activated charcoal. When placed in aqueous solution, the 1.0 M iron solution magnetic biochar is more magnetic than the 0.1 M iron solution magnetic biochar. This indicates that the existence and stability of a magnetic medium is greater in the 1.0 M iron solution magnetic biochar than in the 0.1 M iron solution magnetic biochar. This means that a good magnetic separation method can be used to get powdered magnetic biochar after it has been used.

Concentration (molarity)	Absorbance (%)
0.05 M	0.0273159
0.1 M	0.0525201
0.2 M	0.0877593
0.4 M	0.158808

Table 1 Concentrations of iron (II) chloride solutions and its absorbance values

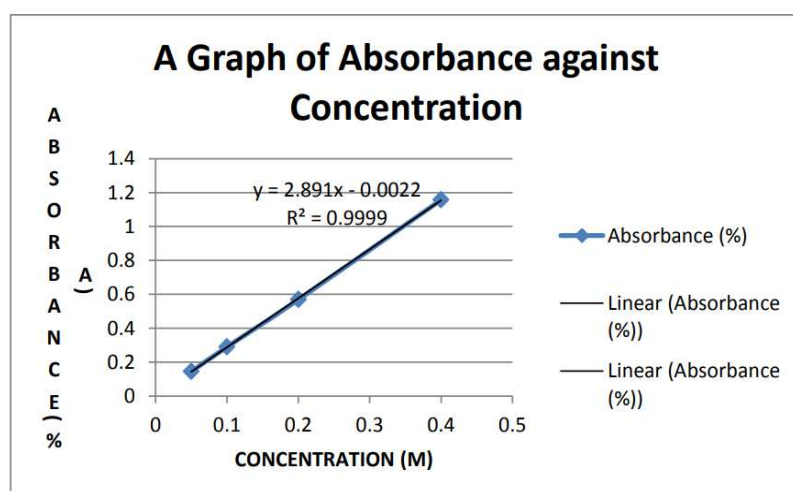


Graph1 A calibration graph of absorbance against concentration for iron (II) chloride solution

Concentration (molarity)	Absorbance (%)
0.05	0.144641
0.1	0.28928
0.2	0.5685
0.4	1.157115

Table 2 Concentrations of iron (III)

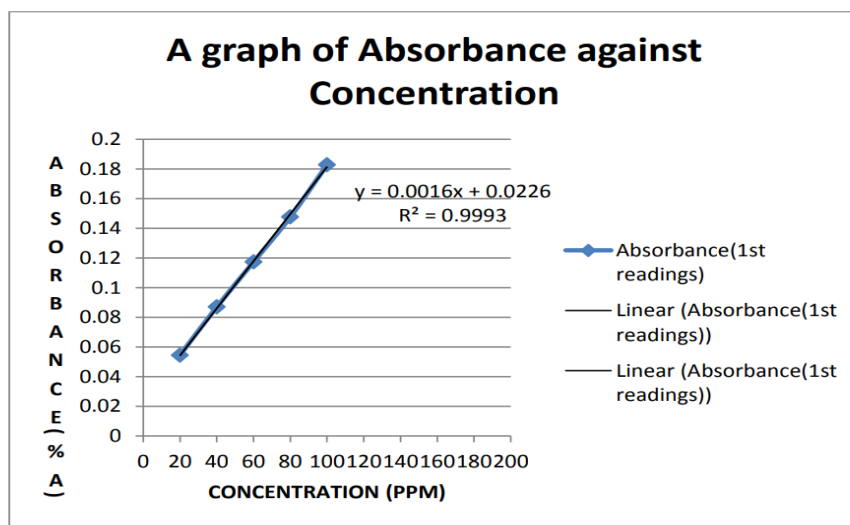
chloride solutions and its absorbance values from U V/VIS spectrometry analysis



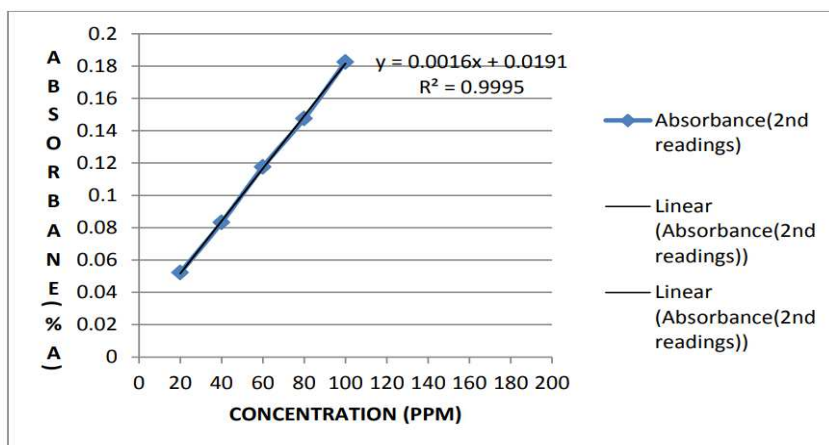
Graph 2 A calibration graph of absorbance against concentration for iron (III) chloride solution

Concentration (ppm)	Absorbance (1st readings)(%)	Absorbance (2nd readings) (%)	Absorbance (3rd readings) (%)	Average readings (%)
20ppm	0.054447	0.0522312	0.0517645	0.052814233
40ppm	0.0869189	0.083149	0.087423	0.0858303
60ppm	0.11723	0.117526	0.117971	0.117575667
80ppm	0.14756	0.147477	0.147971	0.147669333
100ppm	0.182753	0.182508	0.183001	0.182754
200ppm	0.283956	0.283908	0.28405	0.283971333

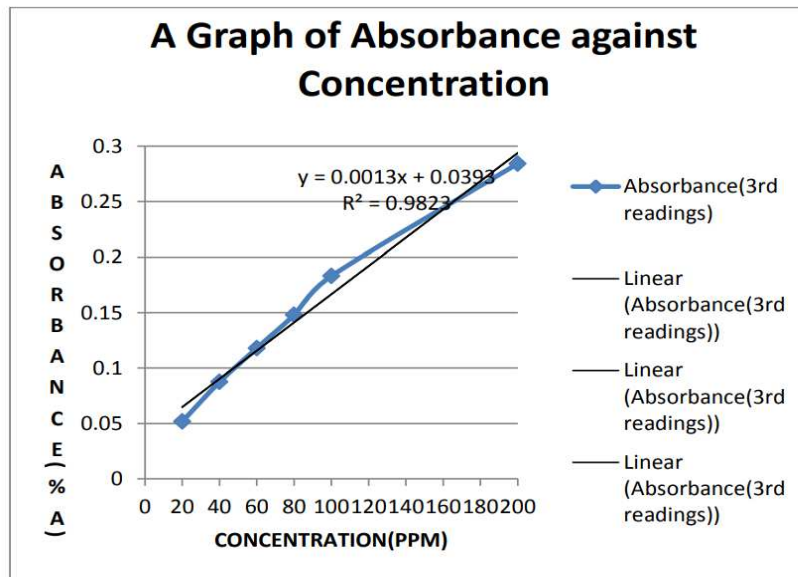
Table 3 Concentration of copper (II) sulphate pentahydrate in 2% Nitric acid standard solution and its absorbance repeated and average values from spectra measurement method from JASCO V-630 U V/VIS spectrophotometer



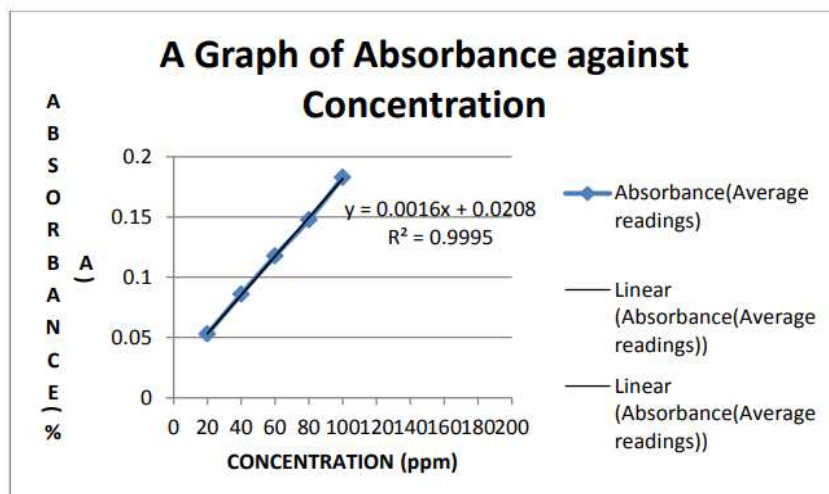
Graph 3 A calibration graph of absorbance (1st reading) against concentration of copper (II) sulphate pentahydrate with 2% Nitric acid standard solutions for spectra measurement



Graph 4 A calibration graph of absorbance (2nd readings) against concentration of copper (II) sulphate pentahydrate with 2% Nitric acid standard solutions for spectra measurement



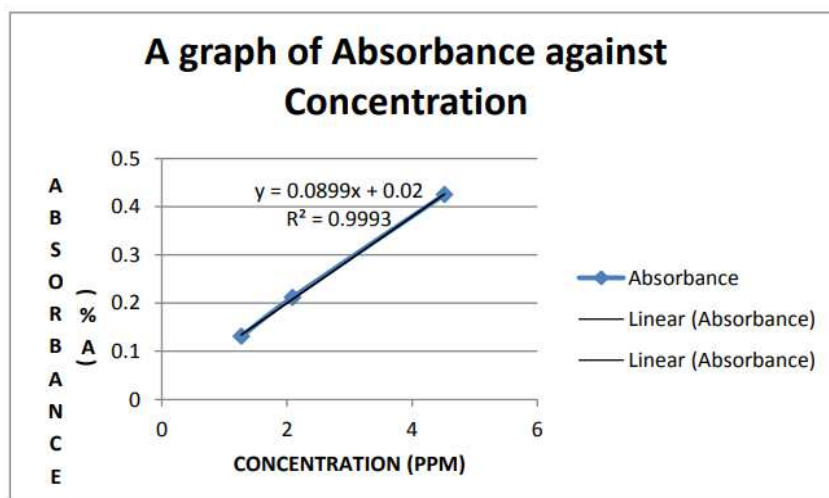
Graph 5 A calibration graph of absorbance (3rd readings) against concentration of copper (II) sulphate pentahydrate with 2% Nitric acid standard solutions for spectra measurement



Graph 6 A calibration graph of absorbance (average readings) against concentration of copper (II) sulphate pentahydrate with 2% Nitric acid standard solutions for spectra measurement

Concentration(ppm)	Absorbance (%)
1.2716	0.131
2.0888	0.212
4.519	0.425

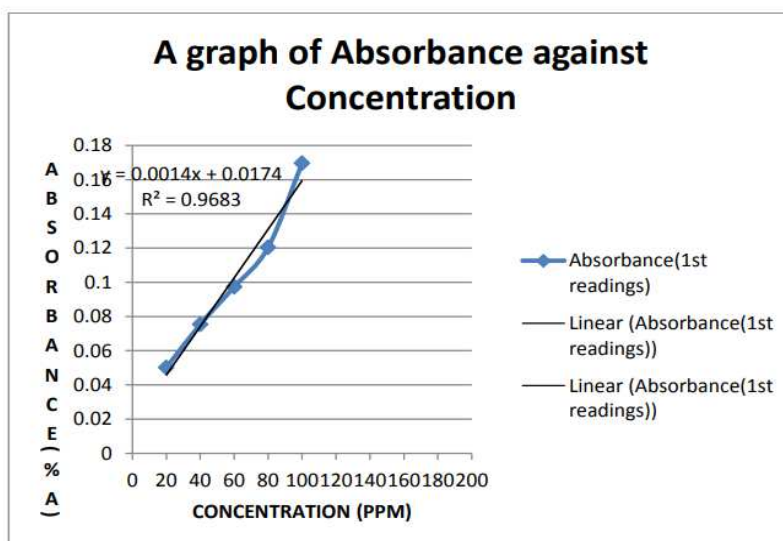
Table 4 Concentrations of copper (II) sulphate pentahydrate and its absorbance values using Atomic absorption spectrometer



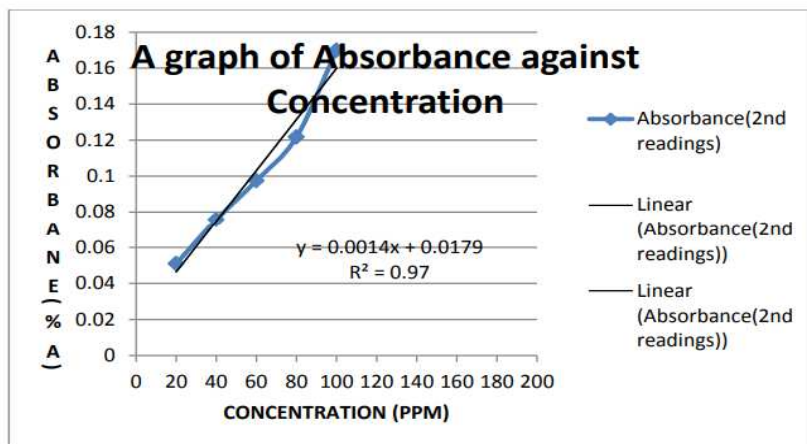
Graph 7 A calibration graph of absorbance against concentration of copper (II) sulphate pentahydrate with 2% Nitric acid standard solutions using Atomic absorption spectrometer

Concentration(ppm)	Absorbance (1st readings)	Absorbance (2nd readings)	Absorbance (3rd readings)	Absorbance (average readings)
20ppm	0.0501	0.0509	0.051	0.050666667
40ppm	0.0754	0.0757	0.0758	0.075633333
60ppm	0.0973	0.0975	0.0978	0.097533333
80ppm	0.1204	0.1217	0.1228	0.121633333
100ppm	0.1696	0.1699	0.175	0.1715
200ppm	0.2633	0.2637	0.2668	0.2646

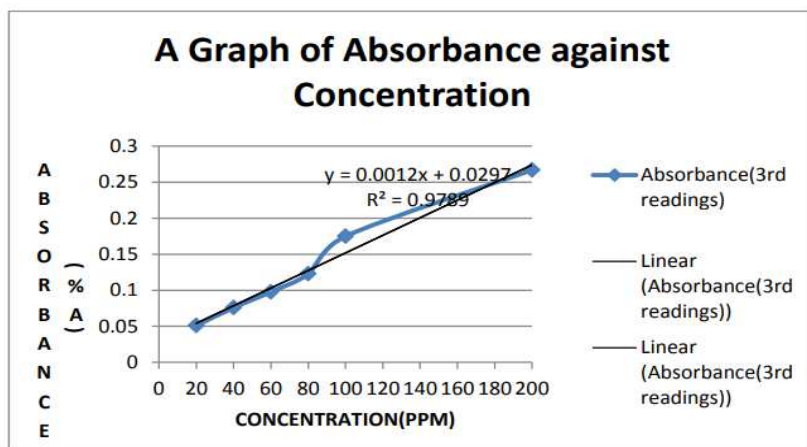
Table 5 Concentration of copper (II) sulphate pentahydrate in 2% Nitric acid standard solution and its absorbance repeated and average values from fixed wavelength measurement method from JASCO V-630 U V/VIS spectrophotometer



Graph 8 A calibration graph of absorbance (1st readings) against concentration of copper (II) sulphate pentahydrate with 2% Nitric acid standard solutions for fixed wavelength measurement



Graph 9 A calibration graph of absorbance (2nd readings) against concentration of copper (II) sulphate pentahydrate with 2% Nitric acid standard solutions for fixed wavelength measurement



Graph 10 A calibration graph of absorbance (3rd readings) against concentration of copper (II) sulphate pentahydrate with 2% Nitric acid standard solutions for fixed wavelength measurement

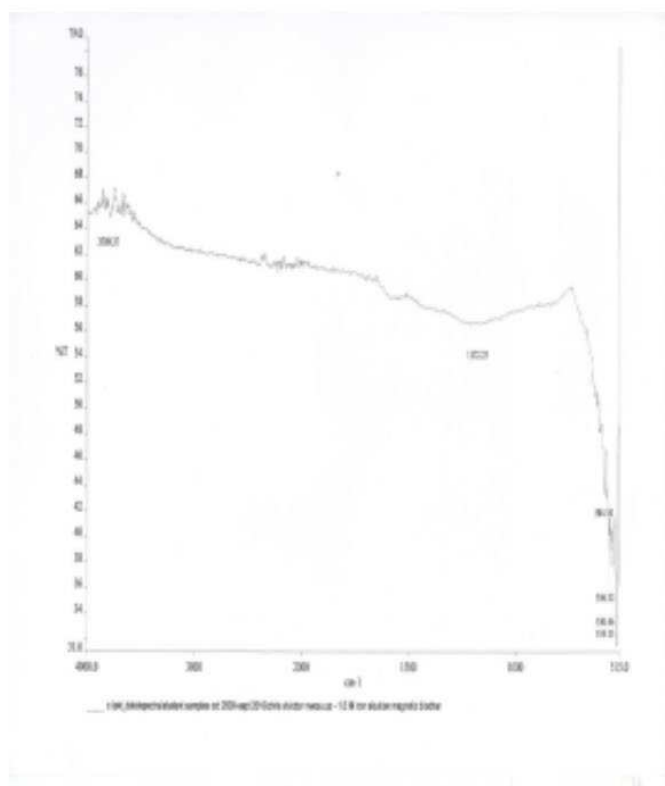


Fig 31 FTIR spectra analysis for 1.0 M iron solution magnetic biochar

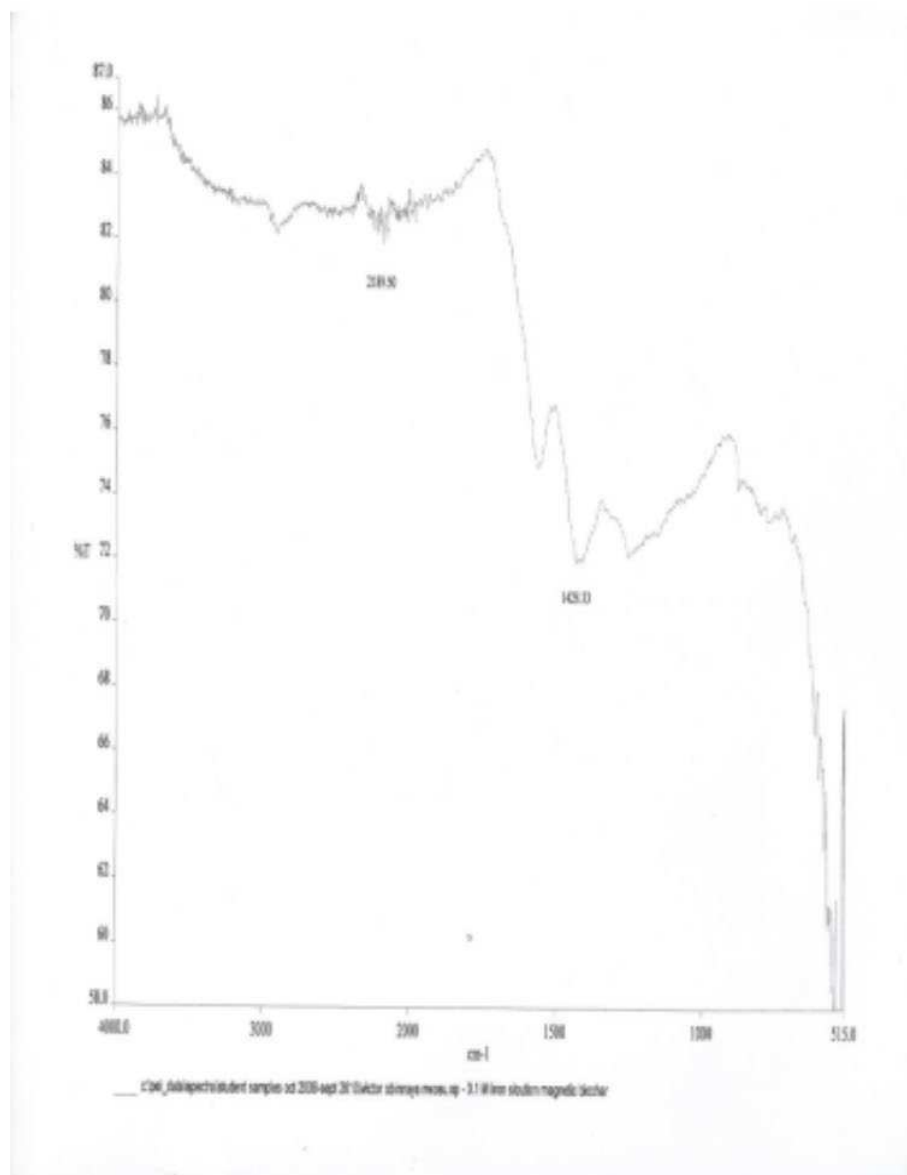


Fig 32 FTIR spectra analysis for 0.1M iron solution magnetic biochar

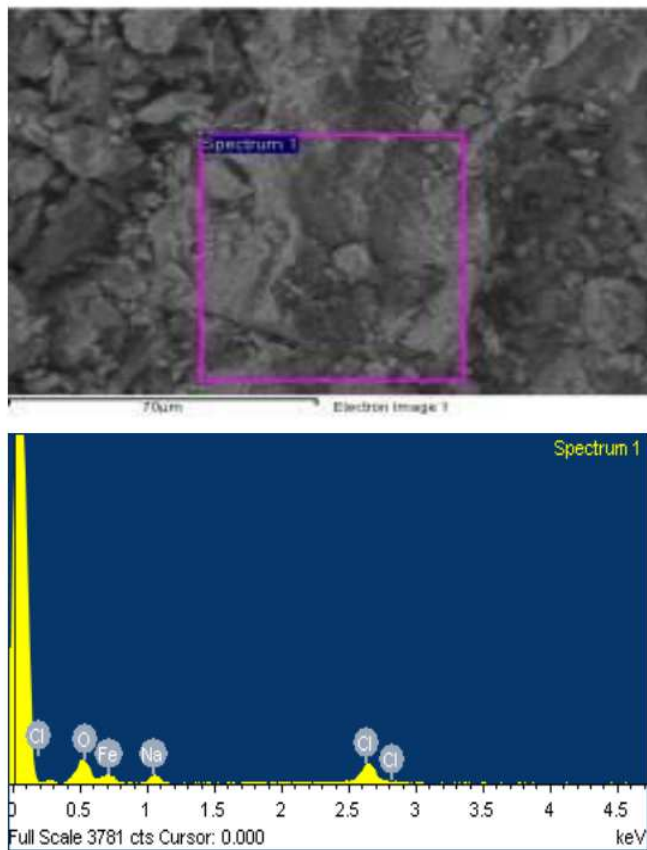


Fig 33 Scanning Electron Microscopy image and spectrum for 1.0 M iron solution magnetic biochar

Element	Weight (%)	Atomic (%)	Compound (%)	Formula
Na K	5.64	8.34	7.6	Na ₂ O
Cl K	7.78	7.46	0	
Fe K	65.77	40.02	84.61	FeO
O	20.81	44.19	0	

Table 6 Elemental compositions for 1.0 M iron solution magnetic biochar

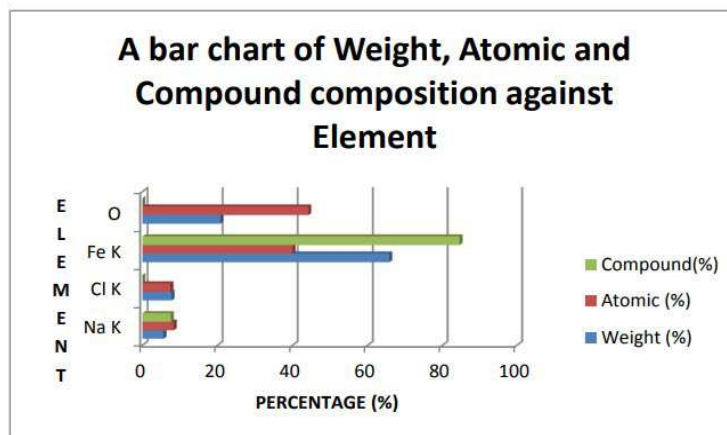
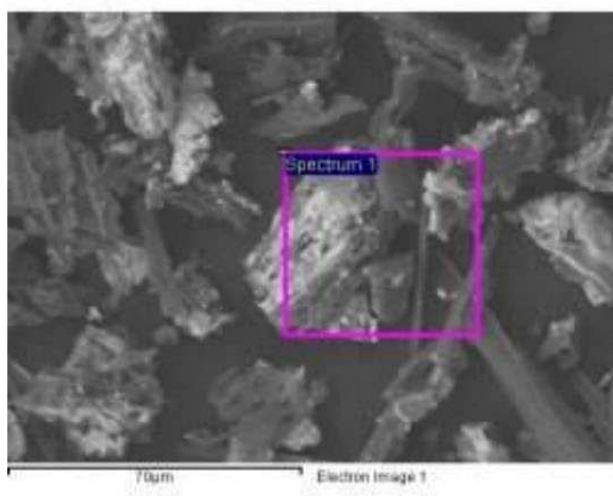


Fig 34 A bar chart of weight, atomic and compound composition against element for 1.0 M iron solution magnetic biochar



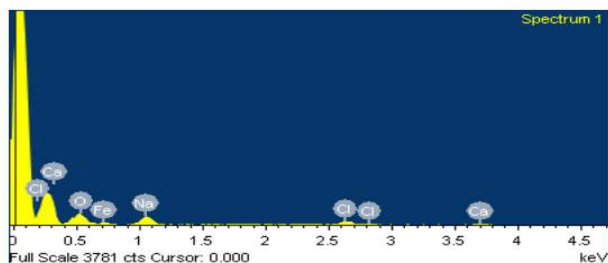


Fig 35 Scanning Electron Microscopy image and spectrum for 0.1 M iron solution magnetic biochar

Element	Weight (%)	Atomic (%)	Compound (%)	Formula
Na K	19.98	25.8	26.94	Na ₂ O
Cl K	5.81	4.87	0	
Ca K	2.66	1.97	3.72	CaO
Fe K	20.81	44.19	63.53	
O	22.16	41.12	0	

Table 7 Elemental compositions for 0.1 M iron solution magnetic biochar

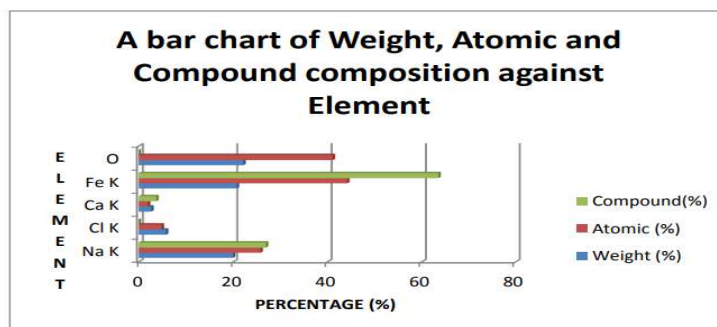
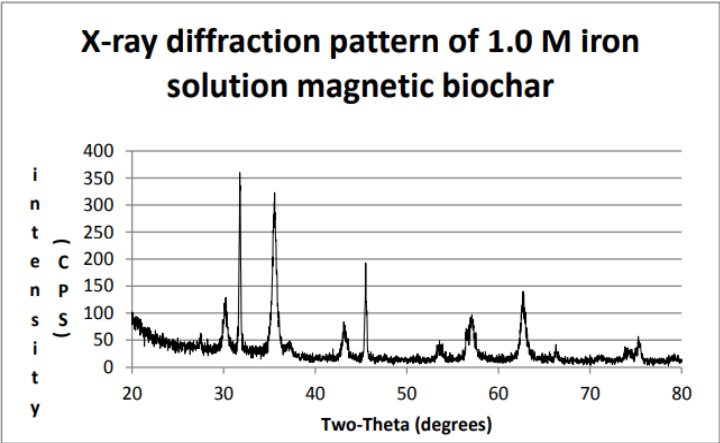


Fig 36 A bar chart of weight, atomic and compound composition against element for 0.1 M iron solution magnetic biochar



Graph 12 X-ray diffraction (XRD) pattern of 1.0 M iron solution magnetic biochar

Sample	Absorbance(1st readings)	Absorbance(2nd readings)	Absorbance(3nd readings)	Absorbance (Average readings)
1ml of deionised water only	0.0222	0.0208	0.0205	0.021166667
10mg of 1.0 M magnetic biochar with 1ml of deionised water	0.0612	0.0616	0.0628	0.061866667
10mg of 1.0 M magnetic biochar with 1ml of 40ppm of copper solution	0.1139	0.1146	0.1143	0.114266667

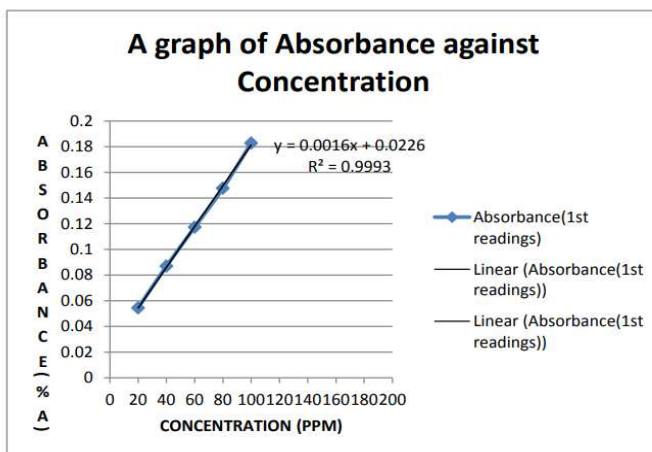
Table 8 Three samples with repeated readings of absorbance values using fixed wavelength measurement

Sample	Absorbance(1st readings)	Absorbance(2nd readings)	Absorbance(3rd readings)	Absorbance (Average readings)
1ml of deionised water only	0.0445459	0.0460592	0.0442495	0.044951533
10mg of 1.0 M magnetic biochar with 1ml of deionised water	0.0610493	0.0625683	0.0647552	0.062790933
10mg of 1.0 M magnetic biochar with 1ml of 40ppm of copper solution	0.134496	0.133765	0.134598	0.134286333

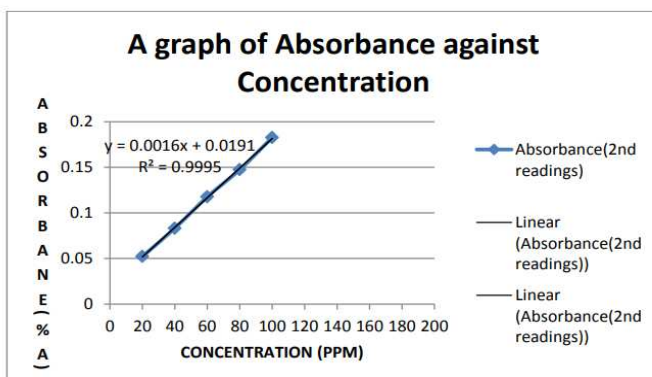
Table 9 Three samples with repeated readings of absorbance values using spectra measurement

Concentration(ppm)	Absorbance(1st readings)	Absorbance(2nd readings)	Absorbance(3rd readings)	Absorbance(Average readings)
20ppm	0.054447	0.0522312	0.0517645	0.052814233
40ppm	0.0869189	0.083149	0.087423	0.0858303
60ppm	0.11723	0.117526	0.117971	0.117575667
80ppm	0.14756	0.147477	0.147971	0.147669333
100ppm	0.182753	0.182508	0.183001	0.182754
200ppm	0.283956	0.283908	0.28405	0.283971333

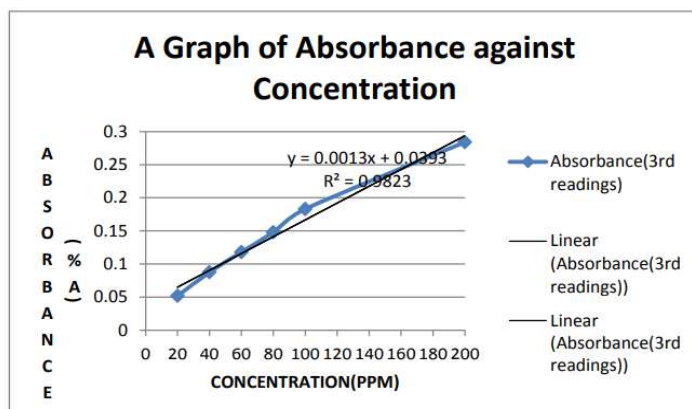
Table 10 Concentration of copper (II) sulphate pentahydrate in 2% Nitric acid standard solution and its absorbance repeated and average values from spectra measurement method from JASCO V-630 U V/VIS spectrophotometer



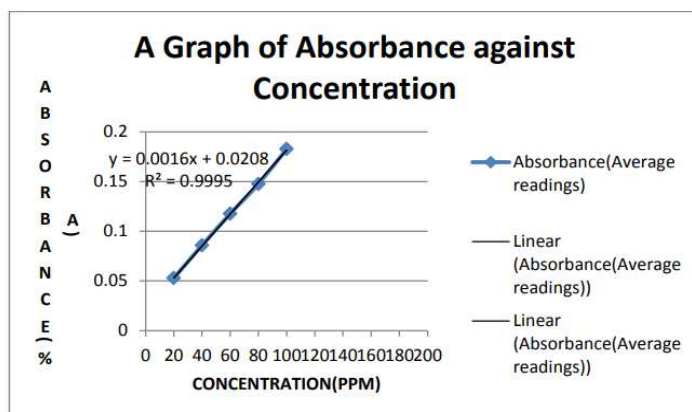
Graph 13 A calibration graph of absorbance (1st readings) against concentration of copper (II) sulphate pentahydrate with 2% Nitric acid standard solutions for spectra measurement



Graph 14 A calibration graph of absorbance (2nd readings) against concentration of copper (II) sulphate pentahydrate with 2% Nitric acid standard solutions for spectra measurement



Graph 15 A calibration graph of absorbance (3rd readings) against concentration of copper (II) sulphate pentahydrate with 2% Nitric acid standard solutions for spectra measurement



Graph 16 A calibration graph of absorbance (average readings) against concentration of copper (II) sulphate pentahydrate with 2% Nitric acid standard solutions for spectra measurement

4.2 ADSORPTION ANALYSIS OF 40PPM OF COPPER (II) SULPHATE PENTAHYDRATE WITH 1.0 M IRON SOLUTION MAGNETIC BIOCHAR

The results from adsorption analysis in terms of absorbance values for the 40ppm of copper (II) sulphate pentahydrate in 2% nitric acid and 1ml (about 0.03 oz) of deionized water mixed with 1.0 M iron solution magnetic biochar; 1ml (about 0.03 oz) of deionized water only are shown above in table 8 and table 9, respectively. The repeated readings absorbance values of copper sulphate solution were much lower than the absorbance values of 10mg (about the weight of a grain of table salt) of 1.0 M iron solution magnetic biochar mixed in 1ml (about 0.03 oz) of 40ppm of copper (II) sulphate pentahydrate standard solution. Also, the repeated readings absorbance values of 1ml (about 0.03 oz) of deionized water are lower than the repeated reading absorbance values of 10mg (about the weight of a grain of table salt) of 1.0 M iron solution magnetic biochar in 1ml (about 0.03 oz) of deionized water which means that for the 1ml (about 0.03 oz) of deionized water; its concentration was increased when 1.0 M iron solution biochar was added and mixed with it, the 1.0 M iron solution magnetic biochar with 1ml (about 0.03 oz) of 40ppm of copper (II) sulphate pentahydrate solution is higher than the 10mg of 1.0 M iron solution magnetic biochar with 1ml (about 0.03 oz) of deionized water. The adsorbed concentration is calculated from the trendline equation for the graph plot points of six concentrations of copper (II) sulphate pentahydrate solution by placing the absorbance value of 10mg (about the weight of a grain of table salt) of 1.0 M iron solution magnetic biochar mixed with 40ppm of copper (II) sulphate pentahydrate solution; for spectra measurement method, the calibration equation of the calibration graph of absorbance plotted against concentration for average readings is

$y=0.0016x+0.0208$ which y is the absorbance and x are the concentration; the absorbance average reading value of 10mg of 1.0 M iron solution magnetic biochar mixed with 1ml of 40ppm of copper (II) sulphate pentahydrate is 0.13428633%A then;

$$0.13428633=0.0016x+0.0208 \dots\dots\dots 1$$

$$0.0016x=0.134286333-0.0208 \dots\dots\dots 2$$

$$0.0016x=0.113486333 \dots\dots\dots 3$$

x=70.9ppm which is the adsorbed concentration of copper (II) sulphate pentahydrate solution. To calculate the adsorbed mass of copper, we first calculate the change in concentration which is shown below:

$$\text{Change in concentration}=70.9\text{ppm}-40\text{ppm}=30.9\text{ppm}=30.9\text{mg/L}$$

$$\text{Adsorbed mass of copper}=0.001\text{L}\times 249.7\text{g/mol}\times 0.0309\text{g/L}=0.007715\text{g or } 7.715\text{mg}$$

$$\begin{aligned} \text{Adsorption capacity} &= \text{adsorbed mass of copper} / \text{mass of 1.0 M iron solution magnetic} \\ \text{biochar used} &= 0.007715\text{g} / 0.01\text{g} = 0.7715\text{g/g} \end{aligned}$$

For the fixed wavelength measurement, the calibration equation of the calibration graph of absorbance plotted against concentration for the 3rd readings is $y=0.0012x+0.0297$ which y is the absorbance on the y-axis and the x is the concentration on the x-axis; the absorbance 3rd reading value of 10mg of 1.0 M iron solution magnetic biochar added and mixed with 1ml of 40ppm of copper (II) sulphate pentahydrate solution is

$$0.11426667\%$$

A then:

$$0.11426667=0.0012x+0.029\dots\dots\dots 1$$

$$0.0012x=0.11426667-0.029$$

$$\dots\dots\dots 2$$

$$0.0012x=0.08526667$$

$$\dots\dots\dots$$

3

X=71.1ppm which is the adsorbed concentration of copper (II) sulphate pentahydrate

solution. For the calculation of the adsorbed mass of copper, we calculate the concentration change which is shown below:

Change in concentration= $71.1\text{ppm}-40\text{ppm}=31.1\text{ppm}$ or 31.1mg/L

Adsorbed mass of copper= $0.001\text{L}\times 249.7\text{g/mol}\times 0.0311\text{g/L}=0.00776567\text{g}$ or 7.76567mg

Adsorption capacity= $0.00776567\text{g}/0.01\text{g}=0.776567\text{g/g}$

The adsorbed mass of copper and adsorbed capacity for the fixed wavelength

measurement is higher than the adsorbed mass of copper and adsorbed capacity for the spectra measurement.

5.0 CONCLUSION AND SUGGESTIONS FOR FURTHER WORK

5.1 CONCLUSION

The iron (II) chloride solution, the iron (III) chloride solution, and SRC willow, which is the agricultural biomass used, can be combined to make 1.0 M iron solution magnetic biochar and 0.1 M iron solution magnetic biochar, respectively; ultra-violet infrared spectrometry was performed on four different concentrations of iron (II) and iron (III) chloride, as well as for six different concentrations of copper (II) sulphate pentoxide. Results from Fourier transform infrared show that 1.0 M iron solution magnetic biochar contains more iron oxide than 0.1 M iron solution magnetic biochar; results from scanning electron microscopy show that there is higher reflectance when light from the microscope is beamed on 1.0 M iron solution magnetic biochar than on 0.1 M iron solution magnetic biochar; and results from X-ray diffraction show that 1.0 M iron solution magnetic biochar contains a high level of iron compounds; both magnetic biochar's contain iron. According to the results of atomic absorptive spectrometry, the adsorption capacity of 1.0 M iron solution magnetic biochar is significantly lower than that of 0.1 M iron solution magnetic biochar. On the other hand, according to the results of ultra-violet infrared spectrometry, the absorption capacity of 1.0 M iron solution magnetic biochar is significantly higher than that of 0.1 M iron solution magnetic biochar. The results of the physical and chemical analyses of 1.0 M iron solution magnetic biochar and 0.1 M iron solution magnetic biochar made from SRC willow show that these biochar's have the potential to be used as adsorptive materials for land remediation of metallic toxins and agricultural applications.

5.2 SUGGESTIONS FOR FURTHER WORK

It is recommended that a sorption isotherm be performed on both 1.0 M iron solution magnetic biochar and 0.1 M iron solution magnetic biochar to identify the equilibrium of the sorption of magnetic biochar's at the surfaces of magnetic biochar's when the temperature is held constant. Not only should a sorption study of the magnetic biochar be done on metallic compounds but also on non-metallic compounds. This is so that the quantity of component (i.e., a non-metallic compound) that can be adsorbed, and the adsorption capacity of the magnetic biochar can both be determined. When creating a magnetic biochar with SRC willow, iron carbide should be used rather than iron chloride because iron carbide is ferromagnetic, resistant to chemicals, forms a hard coating, and is a good metallic conductor. On the other hand, iron chloride is not magnetic and can be broken down by compounds like copper.

To find out how the pore sizes of the magnetic biochar's are described, the pore size distribution must be done on the magnetic biochar's. To establish the measure of how exposed the area of the magnetic biochar's is to the size of the pores in the magnetic biochar, the surface area and average pore radius should be determined for the magnetic biochar. This may be done by conducting tests.

REFERENCES

A novel magnetic biochar efficiently sorbs organic pollutants and phosphate. Baoliang Chen, Zaiming Chen, Shaofang Lv. 2010. Zhejiang: Elsevier Limited, 2010, Vol. 102. ISBN.

A review on biomass as a fuel for boilers. Saidur R, Abdelaziz E A, Demirbas A, Hossain M. S and Mekhilef S. 2011. 5, Kuala Lumpur: Elsevier Ltd, 2011, Vol. 15. ISBN.

Abubakar, Muhammad Fadhil Bin. 2010. Atomic Absorption Spectrometry Determination of Copper (Cu) in AAS. Scribd. [Online] 28 January 2010. [Cited: 12 August 2011.] <http://www.scribd.com/doc/25984748/Determination-of-Copper-by-AAS>.

2006. Amazonian Dark Earth Terra Preta. All I Need. [Online] 16 March 2006. [Cited: 20 June 2011.] www.theallineed.com/ecology/06031607.htm.

Amendment of Acid Soils with Crop Residues and Biochar. Jin-Hua YUAN, Ren-Kou XU, Ning WANG and Jiu-Yu LI. 2011. 3, Beijing and Nanjing: Elsevier Ltd, 2011, Vol. 21. ISBN.

An Assessment of U(VI) removal from groundwater using biochar produced from hydrothermal carbonisation. Kumar Sandeep, Vijay A Loganathan, Ram B Gupta and Mark O Barnett. 2011. Norfolk: Elsevier Ltd, 2011. ISBN.

Application of bifunctional magnetic adsorbent to adsorb metal cations and anionic dyes in aqueous solution. Lin Ya-Fen, Hua-Wei Chen, Poh-Sun Chien, Chyow-San Chiou and Cheng-Chung Liu. 2010. Taiwan: Elsevier B.V, 2010, Journal of Hazardous Materials, Vol. 115, pp. pp1124-1130. ISBN.

Arsenic adsorption by magnetic adsorbent CuFe_2O_4 . Rongcheng Wu, Jiuhui Qu and Chengqiang Wu. 2003. 5, Beijing: Research Gate, 2003, Vol. 24. ISBN.

Backer, Teshler I, Souleimanov A and Smith D L. 2011. Biochar for improved N fertilizer efficiency and reduced drought symptoms in corn? Nitrogen. [Online] 2011.

[Cited: 23 July 2011.] http://nitrogen.ceh.ac.uk/nitrogen2011/_poster_presentations/S9_Backker.pdf.

Bennington, J Bret. 2009. The Carbon Cycle and Climate Change. [PDF Document] 1, Canada: Brooks/Cole Production, 2009. ISBN.

Biochar Application to Soil: Agronomic and Environmental Benefits and Unintended Consequences. Kookana R.S, Sarmah A.K, Van Zwieten L, Krull E and Singh B. 2011. South Australia: Elsevier Inc., 21 June 2011, Vol. 112, pp. pp103-143. ISBN.

Biochar based solid acid catalyst for biodiesel production. Amir Mehdi Dehkhoda, Alex H West and Naoko Ellis. 2010. 2, Vancouver: Elsevier B.V, 2010, Vol. 382. ISBN.

Biochar Then and Now. Sustainable Obtainable Solutions. [Online] [Cited: 15 June 2011.] www.s-o-solutions.org/1IPBiocharthen&Now_v5.pdf.

2011. Biochar is used in soils. Biochar International. [Online] 2011. [Cited: 02 July 2011.] <http://www.biochar-international.org/biochar/soils>.

Biocrude oils from the fast pyrolysis of poultry litter and hardwood. Agblevor F.A, Beis S, Kim S.S, Tarrant R and Mante N.O. 2009. 2, Blacksburg: Elsevier Ltd, 2009, Vol. 30. ISBN.

Biosorbents prepared from wood particles treated with anionic polymer and iron salt: Effect of particle size on phosphate adsorption. Eberhardt, Soo-Hong Min. 2008. 3, Pineville: Elsevier Ltd, 2008, Vol. 99. ISBN.

Biotemplating of Metal Carbide Microstructures: The Magnetic leaf. Schnepf, Wen Yang, Markus Antoniette, and Cristina Giordano. 2010. 37, Potsdam: Wiley-VCH Verlag GmbH & Co. KGaA, Weinheim, 2010, Vol. 49. ISBN.

2006. Black is the new green. Sequestration New Feature. [Online] 18 August 2006. [Cited: 2011 June 17.] [www2.ku.edu/~geography/Current Research/woods/black%20is%20the%20new%20 green.pdf](http://www2.ku.edu/~geography/Current%20Research/woods/black%20is%20the%20new%20green.pdf).

Bracmort, Kelsi S. 2009. Biochar: Examination of an Emerging Concept to Mitigate Climate Change. Congressional Research Service. [Online] 03 February 2009. [Cited: 01 June 2011.] www.assets.opencrs.com/R40186_20090203.pdf.

Bramer. An innovative technology for fast pyrolysis of biomass: -the development of the PyRos reactor. University of Twente. [Online] [Cited: 02 July 2011.] <http://www.utwente.nl/ctw/thw/research/Fuelconv/bramer.pdf>.

Brockhoff, Christians N, 2010. Biochar as a Sand-based Rootzone Amendment. Iowa State University. [Online] 25 March 2010. [Cited: 25 July 2011.] <http://www.ag.iastate.edu/farms/09reports/Horticulture/Biochar.pdf>.

Brownsort P A. 2009. Biomass Pyrolysis Process: Performance Parameters and Their Influence on Biochar System Benefits. University of Edinburgh Library. [Online] 2009. [Cited: 26 July 2011.] <http://www.era.lib.ed.ac.uk/bitstream/1842/3116/1/Brownsort%20PA%20MSc%202009.pdf>.

Characterisation of biochar from hydrothermal carbonisation of bamboo. Daniel Schneider, Marina Escala, Kawin Supawittayayothin and Nakorn Tippayawong. 2011. 4, Zurich and Thailand: International Energy and Environment Foundation, 2011, Vol. 2. ISSN.

Coleman, McElligott K, M. 2009. Biochar Amendments to Forest Soils: Effects on Soil Properties and Tree Growth. The University of Idaho. [Online] May 2009. [Cited: 27 July 2011.] http://forest.moscowfs.wsu.edu/smp/solo/documents/GTs/McElligottKristin_Thesis.pdf.

Contrasted effect of biochar and earthworms on rice growth and resource allocation in different soils. Diana Noguera, Marco Rondon, Kam-Rigne Laossi, Valerio Hoyos, Patrick Lavelle, Maria Helena Cruz de Carvalho and Sebastien Barot.

2010. 7, Paris Cedex 05: Elsevier Ltd, 2010, Vol. 42. ISBN. 2010. Cornell University Centre for a Sustainable Future. Sustainable Future. [Online] 24 May 2010. [Cited: 03 July 2011.] <http://www.sustainablefuture.cornell.edu/grants/attachments/CCSF-AVF-2010-final.pdf>.

CuFe₂O₄/activated carbon composite: a novel magnetic adsorbent for the removal of acid orange II and catalytic regeneration. Zhang G, Qu J, Liu H, Cooper AT and Wu R. 2007. 6, Beijing: U.S. National Library of Medicine, 2007, Vol. 68. ISBN.

DeLuca, Derek M and Gundale M, J. 2009. Biochar Effects on Soil Nutrient Transformation. Wilderness. [Online] 13 January 2009. [Cited: 23 July 2011.] http://wilderness.org/files/Biochar%20Effects%20on%20Soil%20Nutrient%20Transformations_0.pdf.

E, Perez and R, Meyer. FTIR Spectroscopy. IRGAS. [Online] [Cited: 11 August 2011.] http://www.ircas.com/technical_papers/ftir_spectroscopy.pdf.

E-Char is Bio Char for Soil Amendent. New Earth Renewable Energy Inc. [Online] [Cited: 30 June 2011.] <http://www.newearth1.net/downloads/E-Char.pdf>.

Energy Crops Short Rotation Coppice-Willow. Renewable Fuels. [Online] [Cited: 28 August 2011.] <http://www.renewablefuels.co.uk/downloads/ENERGY.pdf>.

Ernsting, Smolker A. 2009. Biochar- A Straategy to Adapt/Mitigate Climate Change? Food and Agriculture Organisation of United Nations. [Online] Feburary 2009. [Cited: 23 July 2011.] http://www.fao.org/fileadmin/templates/rome2007initiative/NENA_Forum_2009/Factsheets/FAO_CC Factsheet_Biochar.pdf.

2010. Experiment 13. X-ray Diffraction. The University of Sydney. [Online] 18 February 2010. [Cited: 06 August 2011.] http://www.physics.usyd.edu.au/pdfs/current/sphys/3yr_lab/Expt_13.pdf.

F, Wong and R, Cheung. pKa of a dye: UV-VIS Spectroscopy. Tripod. [Online] [Cited: 07 August 2011.] http://ishigirl.tripod.com/pchem/pka_sample..

F.Verheijen, S. Jeffery, A.C. Bastos, M. van der Velde, I. Diafas. 2010. Biochar Application to Soils. European Commission Joint Research Centre. [Online] 2010. [Cited: 01 June 2011.] www.eusoils.jrc.ec.europa.eu/esdb_archive/eusoils.../EUR24099.pdf.

Heavy Metal Removal from Soils Using Magnetic Seperation: 1. Laboratory Experiments. Nan Feng, Gabriel Bitton, Philip Yeager, Jean-Claude Bonzongo and Ali Bourlariah. 2007. 4, Morocco: Wiley-VCH Verlag GmbH and Co. KGaA, Weinheim, 2007, Vol. 35. ISBN.

Honcho, Head. 2010. Biochar Production History. Socal Biochar. [Online] 23 November 2010. [Cited: 18 June 2011.] www.socalbiochar.com/index.php/history.html.

How is Biochar made? Sustainable obtainable solutions. [Online] [Cited: 30 June 2011.] http://www.s-o-solutions.org/2IPBiocharProduction_v5.pdf.

Hunt, Josiah, et al. 2010. The Basics of Biochar: A Natural Soil Amendment. College of Tropical Agricultural and Human Resources. [Online] December 2010. [Cited: 01 January 2011.] www.ctahr.hawaii.edu/oc/freepubs/pdf/scm-30.pdf.

Impact of black carbon addition to soil on the determination of soil microbial biomass by fumigation extraction. Durenkamp M, Luo Y and Brookes P.C. 2010. 11, Harpenden and Beijing: Elsevier Ltd, 2010, Vol. 42. ISBN.

Induction of Systemic Resistance in Plants by Biochar, a Soil-Applied Carbon Sequestering Agent. Yigal Elad, Dalia Rav David, Yael Meller Harel, Menahem Borenshtein, Hananel Ben Kalifa, Avner Silber, and Ellen R Graber. 2010. 7, Bet Dagan: The Volcani Centre Agricultural Research Organisation, 2010, Vol. 100. ISBN.

Influence of Pecan Biochar on Physical Properties of Norfolk Loamy Sand. Warren J. Busscher, Jeff M. Novak, Dean E. Evans, Don W. Watts, M.A.S Niandou and Ahmedna, Mohamed. 2010. 1, Washington DC: Lippincott Williams and Wilkins, 2010, Vol. 175. ISBN.

2005. Introduction to Fourier Transform Infrared Spectrometry. Thermo Electron Corporation. [Online] 2005. [Cited: 05 August 2011.] http://www.thermo.com/eThermo/CMA/PDFs/Various/File_52263.pdf.

Johannes, Stephen Joseph. 2009. Biochar for Environmental Management: An Introduction. Biochar International. [Online] 23 February 2009. [Cited: 18 June 2011.] http://www.biochar-international.org/images/Biochar_book_Chapter_1.pdf.

Karve, Simon Shakley, Sarah Carter, Paul Tanger and John Field. 2009. Biochar for Carbon Reduction, Sustainable Agricultural and soil. Final Report for APN Project. [Online] 2009. [Cited: 28 June 2011.] www.apngcr.org/newAPN/activities/.../ARCP2009-12NSY-karve.pdf.

Krull, Dr Evelyn. What is Biochar? Commonwealth Scientific and Industrial Research Organisation. [Online] [Cited: 01 June 2011.] www.csiro.au/files/files/pnzp.pdf.

Laird, Robert Brown, James E Amonette and Johannes Lehmann. 2009. Review of the pyrolysis platform for coproducing bio-oil and biochar. Cornell University. [Online] 2009. [Cited: 02 July 2011.] <http://www.css.cornell.edu/faculty/lehmann/publ/BiofBioproBioref%203,%20547-562,%202009%20Laird.pdf>.

Large-scale biohydrogen production from bio-oil. Kumar, Susanjib Sarkar and Amit. 2010. 19, Aiberta : Elsevier Ltd, 2010, Vol. 101. ISBN.

M, Tarun, et al. 2008. High Purity Water for Atomic Absorption Spectroscopy. Millipore. [Online] 2008. [Cited: 07 August 2011.] [http://www.millipore.com/publications.nsf/a73664f9f981af8c852569b9005b4eee/ae815a6b324c430c8525756900587ccb/\\$FILE/ab2467en00.pdf](http://www.millipore.com/publications.nsf/a73664f9f981af8c852569b9005b4eee/ae815a6b324c430c8525756900587ccb/$FILE/ab2467en00.pdf).

Magnetic dendritic materials for highly efficient adsorption of dyes and drugs. Zhou L, Gao C and Xu W. 2010. Hangzhou: U.S. National Library of Medicine, 2010, Vol. 5. ISBN.

Martin, Lynn Collison, Ruben Sakrabani, Bruce Tofield and Zoe Wallage. 2009. Biochar and Carbon Sequestration: A Regional Perspective. University of East Anglia. [Online] 20 April 2009. [Cited: 01 July 2011.] http://www.uea.ac.uk/polopoly_fs/1.118134!LCIC%20EEDA%20BIOCHAR%20REVIEW%2020-04-09.pdf.

Mesa, Spokas K A, 2006. Impacts of Biochar (Black Carbon) Additions on the Sorption and Efficacy of Herbicides. Intechopen. [Online] 2006. [Cited: 23 July 2011.] http://www.intechopen.com/source/pdfs/12591/InTechImpacts_of_biochar_black_carbon_additions_on_the_sorption_and_efficacy_of_herbicides.pdf.

Meyer, Daniel. 2009. Biochar-A Survey. Lupus 78. [Online] 25 May 2009. [Cited: 20 June 2011.] www.lupus78.de/projekte/uni/biochar.pdf.

Organic arsenic adsorption onto a magnetic sorbent. Lim, Zheng YM and Chen JP. 2009. 9, Singapore: National Centre for Biotechnology Information, U.S. National Library of Medicine, 2009, Vol. 25. ISBN.

Palumbo, Iris Porat, Philips J R, Amonette J E, Drake M M, Brown S D and Schadt C W. 2009. Leaching of Mixtures of Biochar and Fly Ash. Fly Ash. [Online] 7 May 2009. [Cited: 23 July 2011.] <http://www.flyash.info/2009/128-palumbo2009.pdf>.

Preparation of high adsorption capacity biochar from waste biomass. Wu-Jun Liu, Fan-Xin Zeng, Hong Jiang and Xue-Song Zhang. 2011. Guangzhou: Elsevier Ltd, 2011. ISBN.

Quayle, Wendy C. 2010. Biochar potential for soil improvement and soil fertility. IREC Farmer Australia. [Online] Autumn 2010. [Cited: 21 July 2011.] http://www.irec.org.au/farmer_f/pdf_182/Biochar%20_a%20means%20of%20storing%20carbon.pdf.

Rajvanshi. Biomass Gasification. Nariphaltan. [Online] [Cited: 01 July 2010.] http://www.nariphaltan.org/nari/pdf_files/gasbook.pdf.

Reduced plant uptake of pesticides with biochar additions to soil. Xiang-Yang Yu, Guang-Guo Ying and Rai S. Kookana. 2009. 5, Nanjing and Guangzhou: Elsevier Ltd, 2009, Vol. 76. ISBN.

Removal of cationic dyes from aqueous solution using magnetic multi-wall carbon nanotube nanocomposite as adsorbent. Gong Ji-Lai, Bin Wang Guang-Ming Zeng,

Chun-Ping Yang, Cheng-Gang Niu, Qin-Ya Niu, Wen-Jin Zhou and Yin Lang. 2009. 2-3, Changsha: Elsevier B.V, 2009, Vol. 164. ISBN.

Removal of lead from water using biochar prepared from hydrothermal liquefaction of biomass. Zhang, Zhengang Liu and Fu-Shen. 2009. 1-3, Beijing: Elsevier B.V, 2009, Vol. 167. ISBN.

Removal of Phosphate from aqueous solutions by biochar derived from anaerobically digested sugar beet tailings. Yao, Bin Gao, Mandu Inyang, Andrew R Zimmeran, Xinde Cao, Pratap Pullammanapallil and Liuyan Yang. 2011. 1-3, Gainesville: Elsevier Ltd, 2011, Vol. 190. ISBN.

Robert, Wayne Teel, John Marier, Geoff Austin, Tim Clark, and Brandon Dick. 2011. Design, Construction, and Analysis of a Farm-Scale Biochar Production System. NCIIA. [Online] 24 March 2011. [Cited: 15 June 2011.] www.nciia.org/sites/default/files/u7/Prins.pdf.

Rodriguez, Salazar P and Preston T R. 2009. Effect of biochar and biodigester effluent on growth of maize in acid soil. Biochar Bioenergy. [Online] 1 July 2009. [Cited: 24 July 2011.] <http://www.biochar.bioenergylists.org/files/UTALRRD2009.pdf>.

Ruehr, Thomas A. Biological Charcoal is a valuable resource for Agriculture. Earths Answer. [Online] [Cited: 17 July 2011.] http://www.earthsanswer.net/TWA_-_Biochar_Article.pdf.

Safarik, Konstanca Nymburska and Mirka Safarikova. 1996. Adsorption of Water-Soluble Organic Dyes on Magnetic Charcoal. Laboratory of Biochemistry and Biotechnology, Institute of Landscape Ecology, Ceske Budejovice, Czech Republic. [Online] 13 September 1996. [Cited: 10 July 2011.] <http://www.nh.cas.cz/people/safarik/3985.pdf>.

Short-term CO₂ Mineralisation after additions of biochar and switchgrass to a Typic Kandudult. Novak J.M, Busscher W.J, Watts D.W, Laird D.A, Ahmedna M.A and M.A.S Niandou. 2009. 3-4, Florence: Elsevier B.V, 2009, Vol. 154. ISBN.

2008. Significant Climate Mitigation Is Available from Biochar. Institute for Governance and Sustainable Development. [Online] 8 December 2008. [Cited: 17 July 2011.] <http://www.igsd.org/docs/Biochar%20Note%2015%20Dec%202008.pdf>.

Sorption and ecotoxicity of pentachlorophenol polluted sediment amended with rice straw derived biochar. Liping Lou, Binbin Wu, Lina Wang, Ling Luo, Xinhua Xu, Jiaai Hou, Bel Xun, Baolan Hu and Yingxu Chen. 2010. 5, Hangzhou: Elsevier Ltd, 2010, Vol. 102. ISBN.

Sorption of bisphenol A, 17 alpha-ethinyl estradiol and phenathrene on thermally and hydrothermally produced biochars. Sun, Kyoung Ro, Mingxin Guo, Jeff Novak, Hamid Mashayekhi and Baoshan Xing. 2011. 10, Beijing: Elsevier Limited, 17 March 2011, Bioresource Technology, Vol. 102, pp. pp5757-5763. ISBN.

Speeding, Alan. 2010. Biochar. Arthur Rank Centre. [Online] 28 July 2010. [Cited: 17 July 2011.] http://www.arthurrankcentre.org.uk/projects/rusource_briefings/rus10/1088.pdf.

Stadtlander, C.T.K.-H. 2007. Scanning Electron Microscopy and Transmission Electron Microscopy of Mollicutes: Challenges and Opportunities. Modern Research and Educational Topics in Microscopy. [Online] 2007. [Cited: 06 August 2011.] <http://www.the-iom.org/assets/files/SEM-TEM.pdf>.

Talberg, Anita. 2009. The basics of biochar. Parliament Library of Australia. [Online] 10 September 2009. [Cited: 14 June 2011.] www.aph.gov.au/Library/pubs/BN/sci/Biochar.pdf.

The African Biodiversity Network, Biofuelwatch and Gaia Foundation. 2009. Biochar Land Grabbing: the impact on Africa. Biofuel Watch. [Online] November 2009. [Cited: 16 July 2011.] http://www.biofuelwatch.org.uk/docs/biochar_africa_briefing.pdf.

The Kadir Buxton Method. Kadir Buxton. [Online] [Cited: 18 June 2011.] www.kadimbuxton.com/page19.htm.

Topre, Ishan. 2011. Biochar To Replace Activated Carbon Electrodes. Crazy Engineers. [Online] 7 May 2011. [Cited: 23 July 2011.] <http://www.crazyengineers.com/biochar-to-replace-activated-carbon-electrodes-227/>.

Ultraviolet-Visible Spectroscopy Background Information. University of Central Missouri. [Online] [Cited: 06 August 2011.] http://www.ucmo.edu/chemphys/about/documents/cary_300_bio_uv.pdf.

Use of biochar as a bulking agent for the compositing of poultry manure: Effect on organic matter degradation and humification. Dias, Carlos A. Silva, Fabio S Higashikawa, Asuncion Roig and Miguel A. Sanchez-Monedero. 2009. 4, Minas Gerais: Elsevier Limited, 30 September 2009, Vol. 101, pp. pp1239-1246. ISBN.

UV/VIS Spectrometry. Szerves Kémiai Tanszék. [Online] [Cited: 06 August 2011.] <http://szerves.chem.elte.hu/oktatas/ea/Perczel/UV-VIS.pdf>.

X-ray Diffractometer. Dissemination of IT for the Promotion of Materials Science. [Online] [Cited: 14 August 2011.] <http://www.doitpoms.ac.uk/>.

